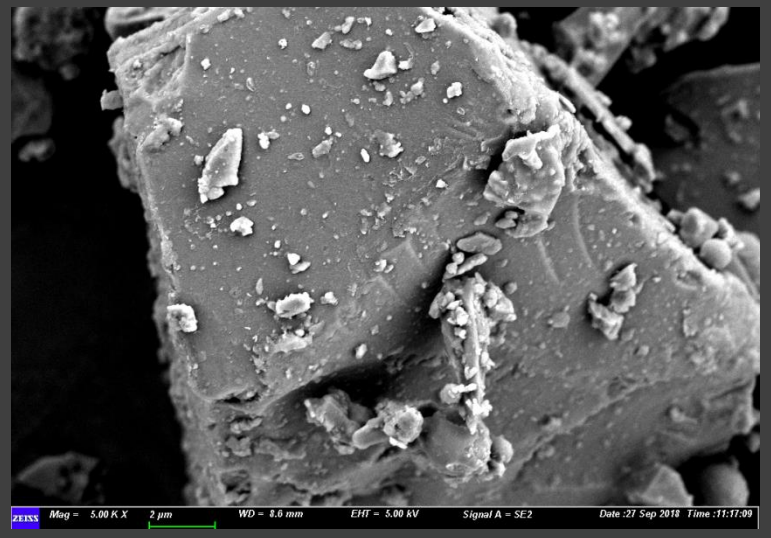

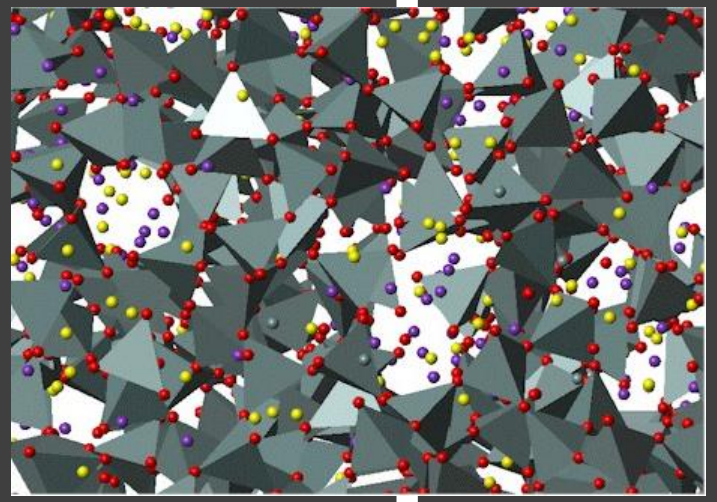

On the Reactivity Mechanism of Supplementary Cementitious Materials by Alkali Activation

Yu Jin Ph.D, Shenzhen Institute of Information Technology

CONTENTS

1 Background

2 Methods

3 Results

4 Conclusions

CONTENTS

1 Background

2 Methods

3 Results

4 Conclusions

Cement, Natural Resources and Solid Waste

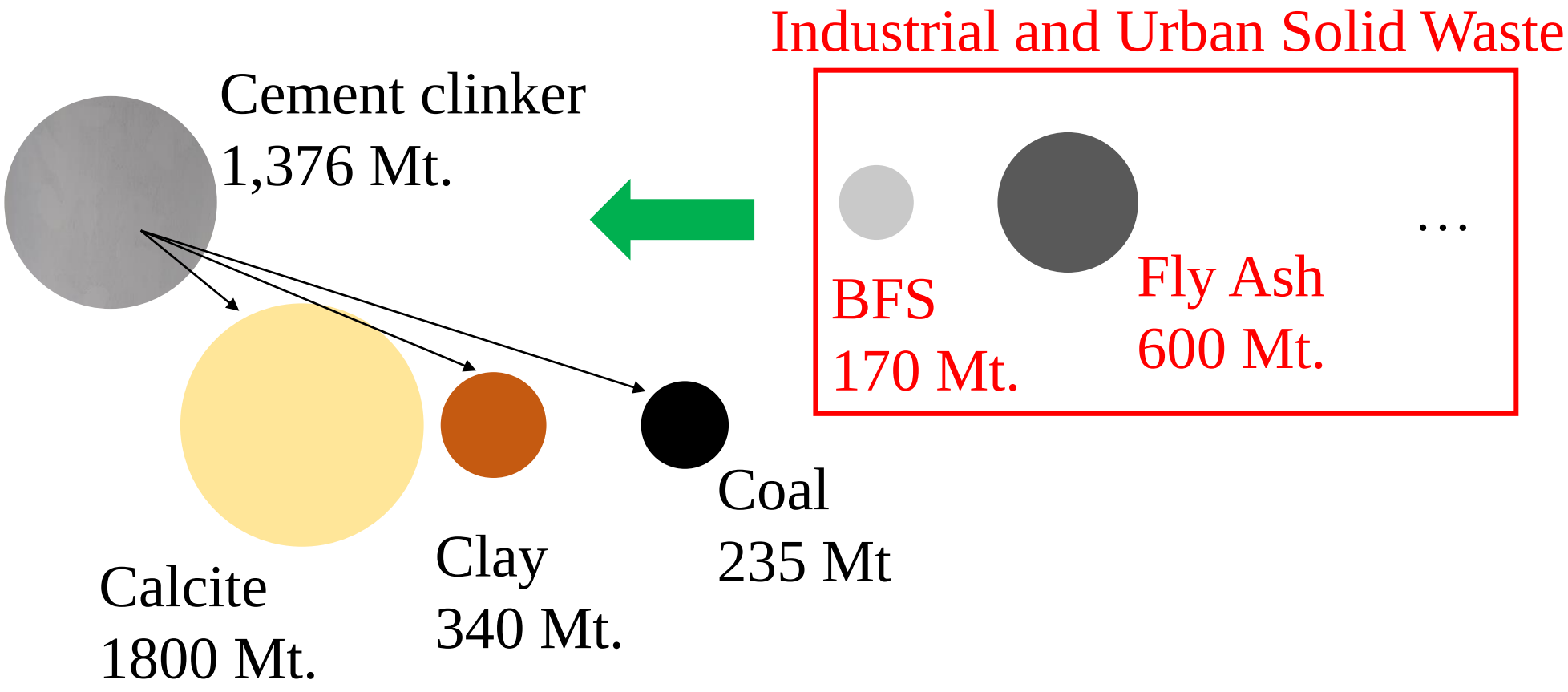

Ground Granulated Blast Furnace Slag

Coal Fly Ash

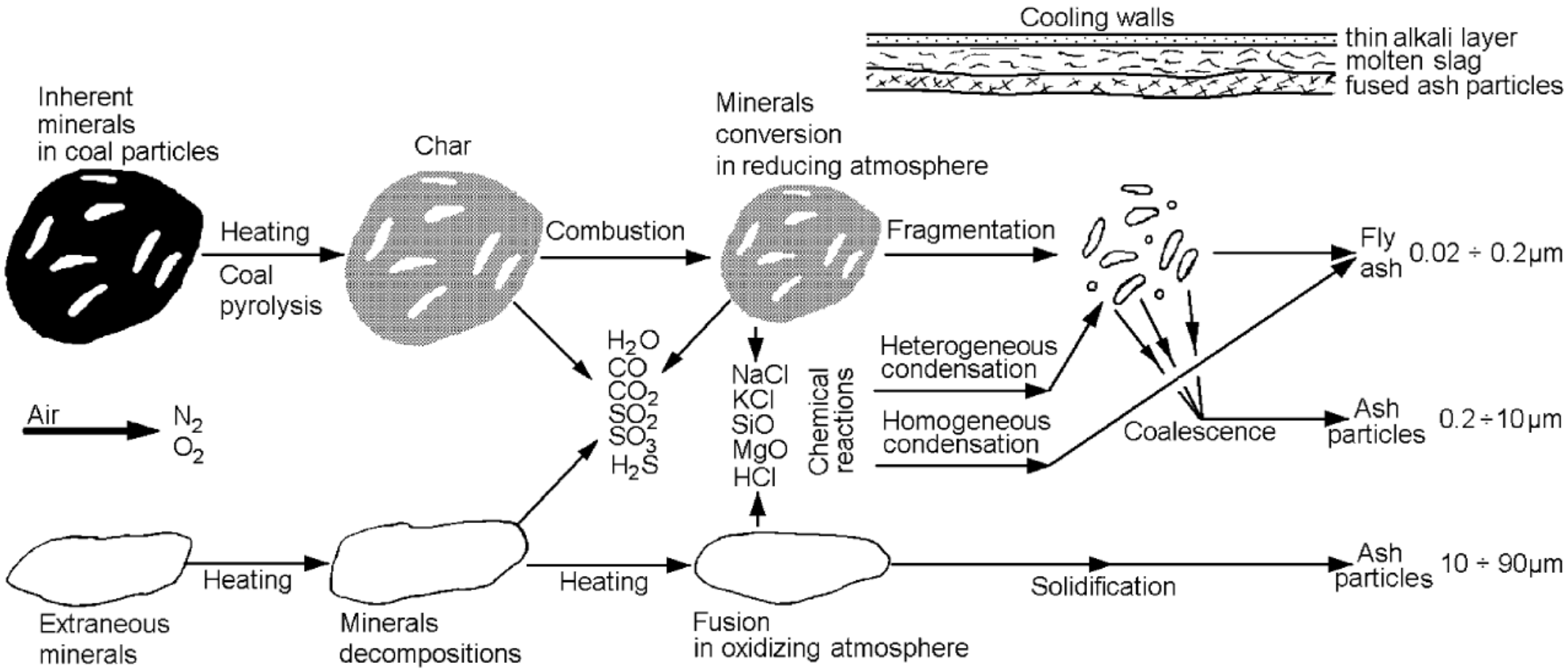

Tomeczek et al. Fuel 2002

Glass Structure of SCM

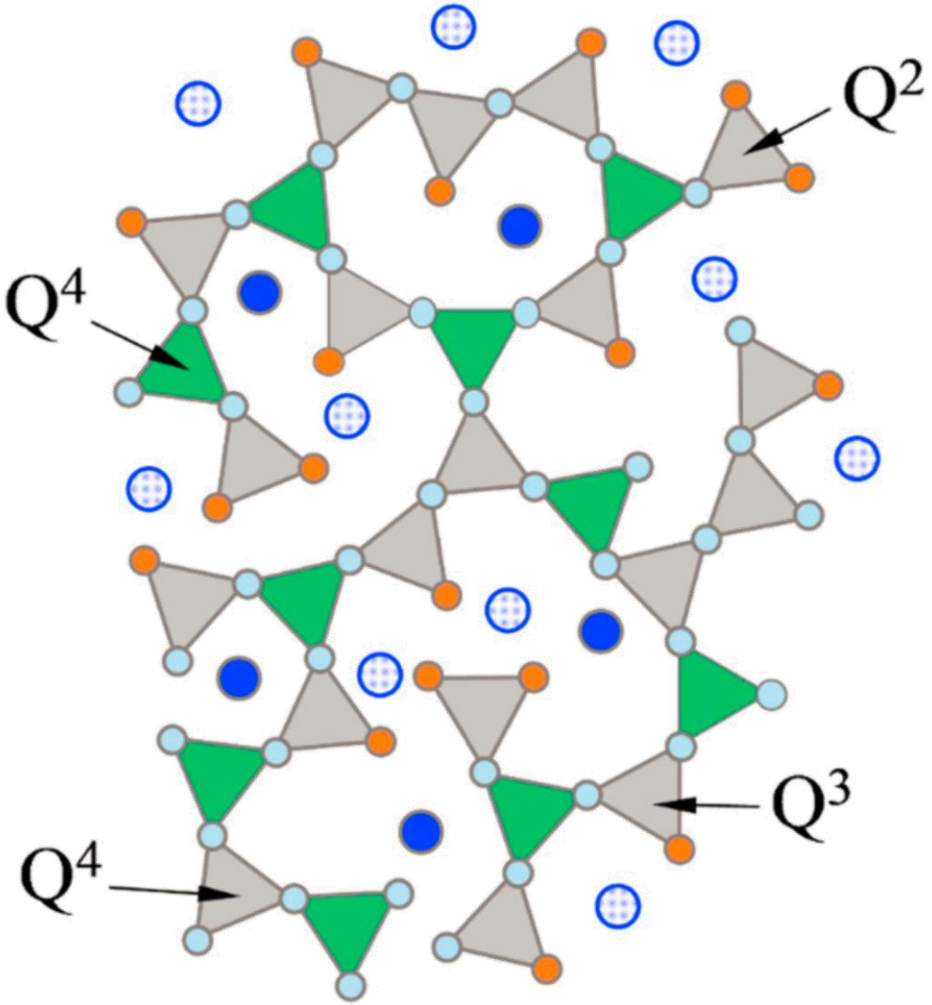

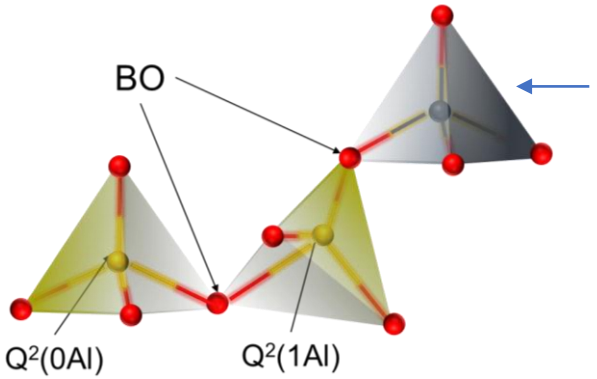

Si^{4+} replaced by Al^{3+} is compensated by alkali cations

Si
Al
O

Network Former

SiO_4 AlO_4

BO Network Modifier

NBO Charge Compensator

Skibsted et al. CCR 2019

Aluminosilicate Glass Dissolution at high pH

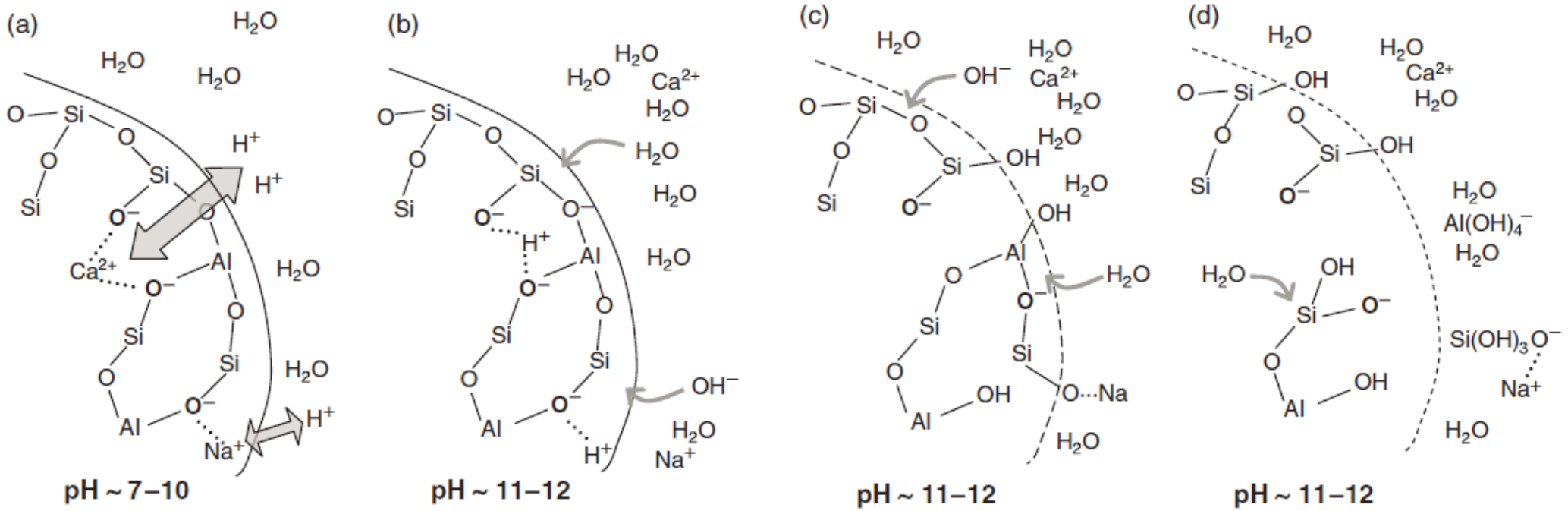

Duxson et al. JACers 2008

Glass Structure and Reactivity

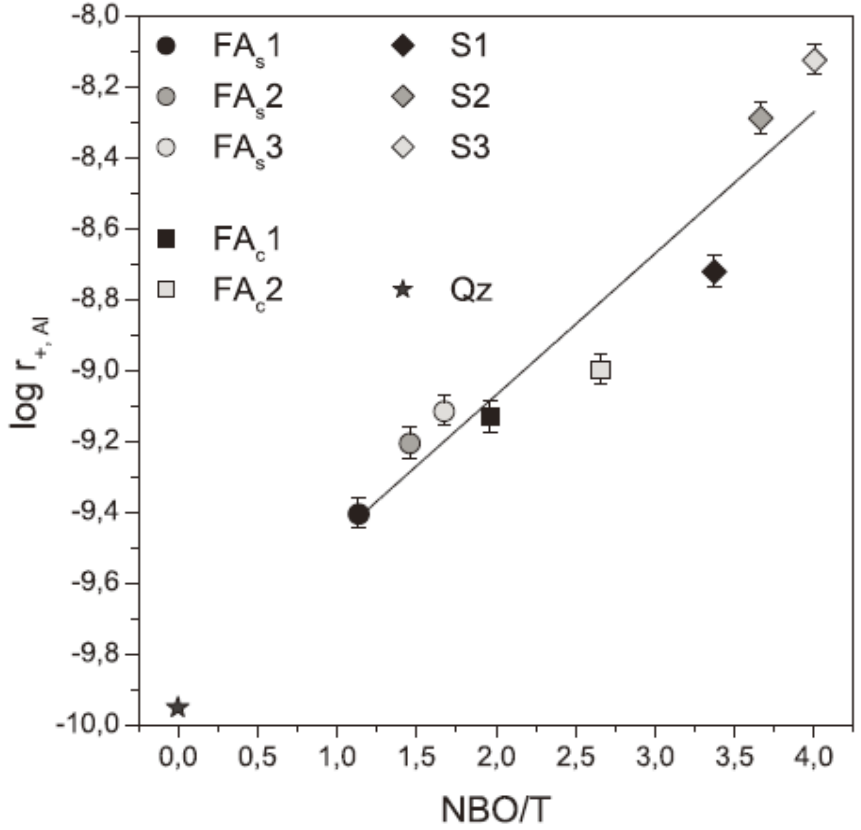

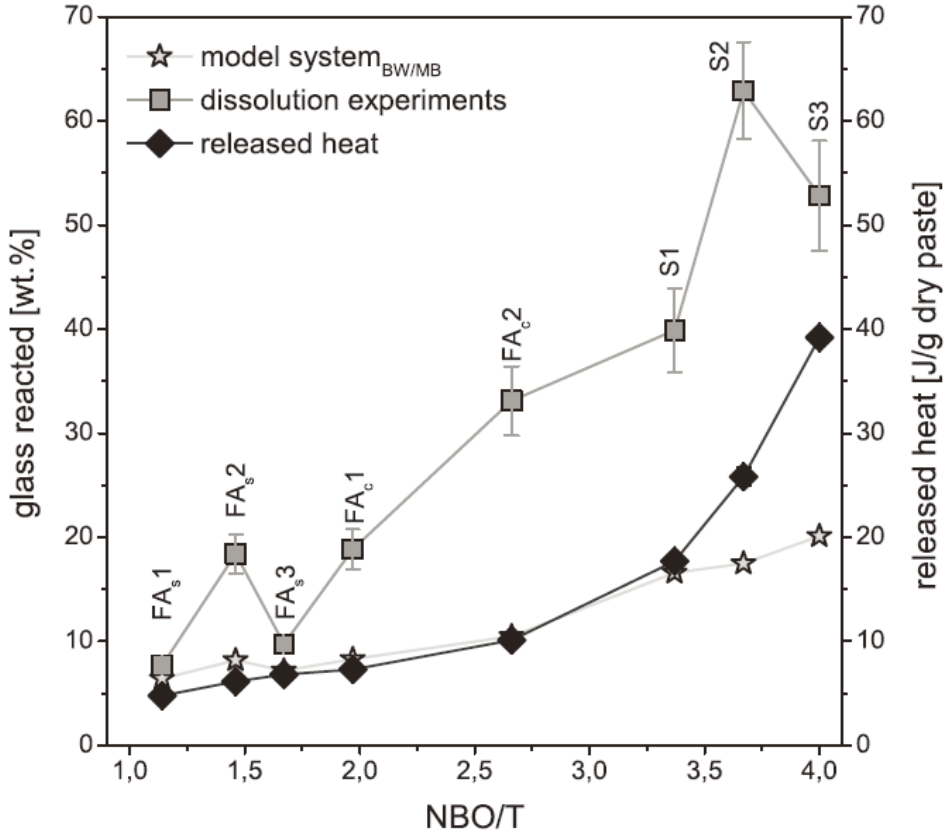

$$\mathrm{NBO/T} = \frac{2(\mathrm{CaO} + \mathrm{MgO} + \mathrm{K_2O} + \mathrm{Na_2O} + 3f_{Fe}\mathrm{Fe_2O_3} + 3f_{Al}\mathrm{Al_2O_3} - (1 - f_{Fe})\mathrm{Fe_2O_3} - (1 - f_{Al})\mathrm{Al_2O_3})}{\mathrm{SiO_2} + \mathrm{TiO_2} + 2(1 - f_{Fe})\mathrm{Fe_2O_3} + 2(1 - f_{Al})\mathrm{Al_2O_3}}$$

Schöler et al. JACers 2017

Glass Structure and Reactivity

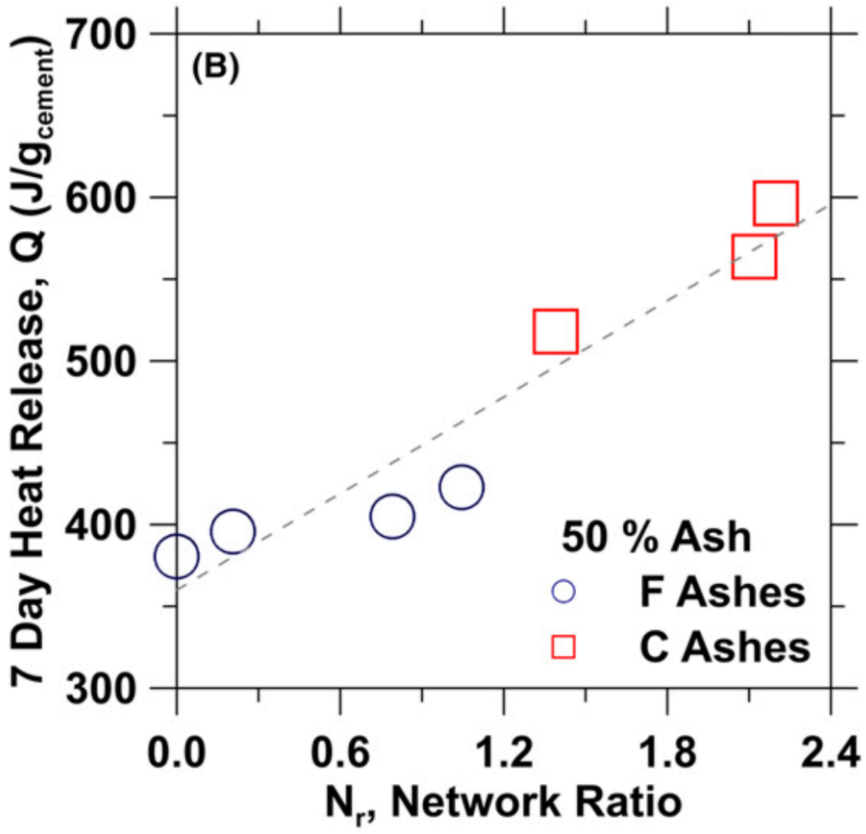

$$N_r = \frac{2 \times (X_{Ca} + X_{Mg}) + X_K + X_{Na} - X_{Al}}{X_{Si} + X_{Al}}$$

$$\text{for } \left[\frac{Al_2O_3}{M_2O + M'O}\right] < 1$$

$$N_r = 0 \text{ for } \left[\frac{Al_2O_3}{M_2O + M'O}\right] > 1$$

Oey et al. JACers 2017

Main Objectives of the Research

1. Refinement of the glass structure of slag and fly ash
2. The correlation between the glass structure and the reactivity
3. The reactivity under various alkali conditions

CONTENTS

1 Background

2 Methods

3 Results

4 Conclusions

Chemical Composition of the slags and fly ashes

	SiO_2	Al_2O_3	Fe_2O_3	TiO_2	CaO	MgO	K_2O	Na_2O	SO_3	L.O.I.
S1	**28.4**	**15.4**	/	1.66	**40.2**	**9.93**	0.40	0.30	3.25	/
S2	**31.9**	**14.5**	/	0.71	**42.8**	**6.71**	0.49	0.42	2.23	/
FA1	**46.1**	**29.0**	**5.0**	0.8	**11.7**	1.9	1.0	0.0	1.9	3.0
FA2	**52.8**	**22.8**	**6.6**	0.8	**11.0**	1.5	1.3	1.4	1.0	3.9
FA3	**51.1**	**34.1**	**3.9**	1.0	**3.8**	1.3	0.8	0.6	0.2	2.8
FA4	**50.4**	**39.1**	**3.1**	1.0	**2.5**	1.1	1.1	0.5	0.6	8.3
FA5	**43.4**	**19.7**	**11.0**	0.7	**15.5**	4.0	1.4	1.5	1.9	1.8

Particle size distribution of the slags and fly ashes

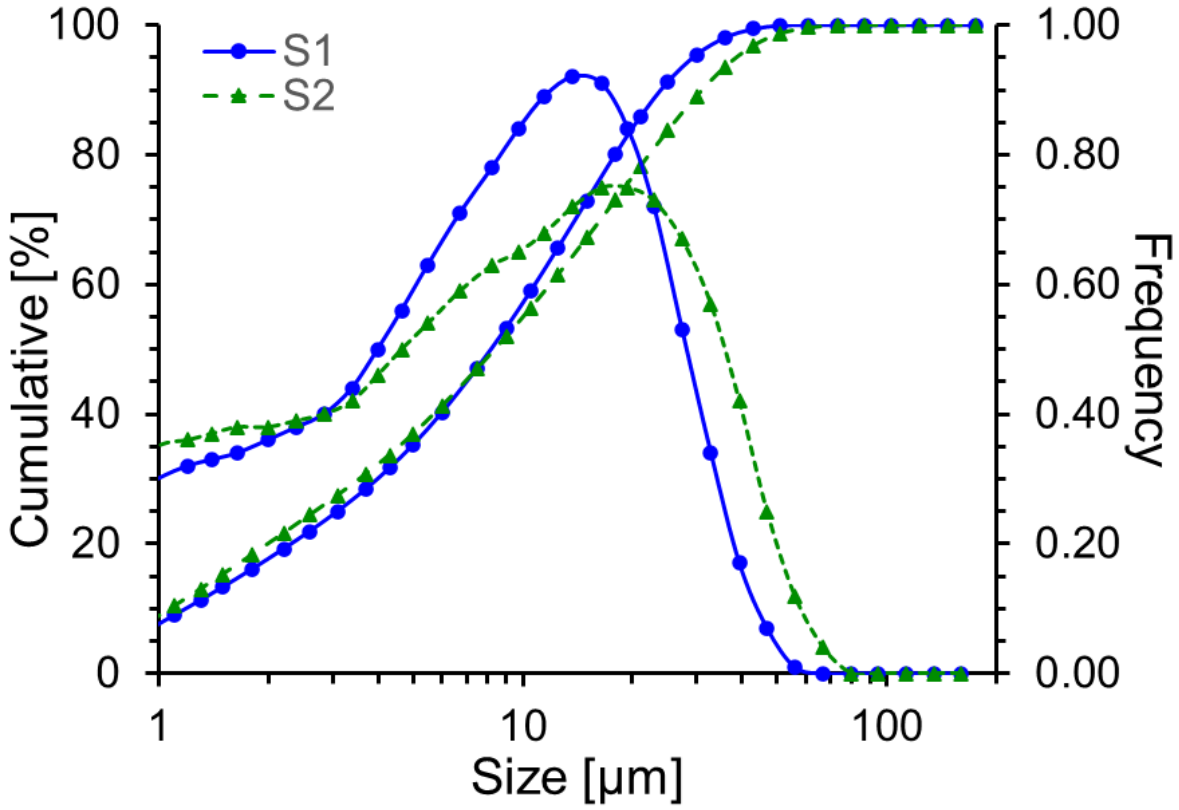

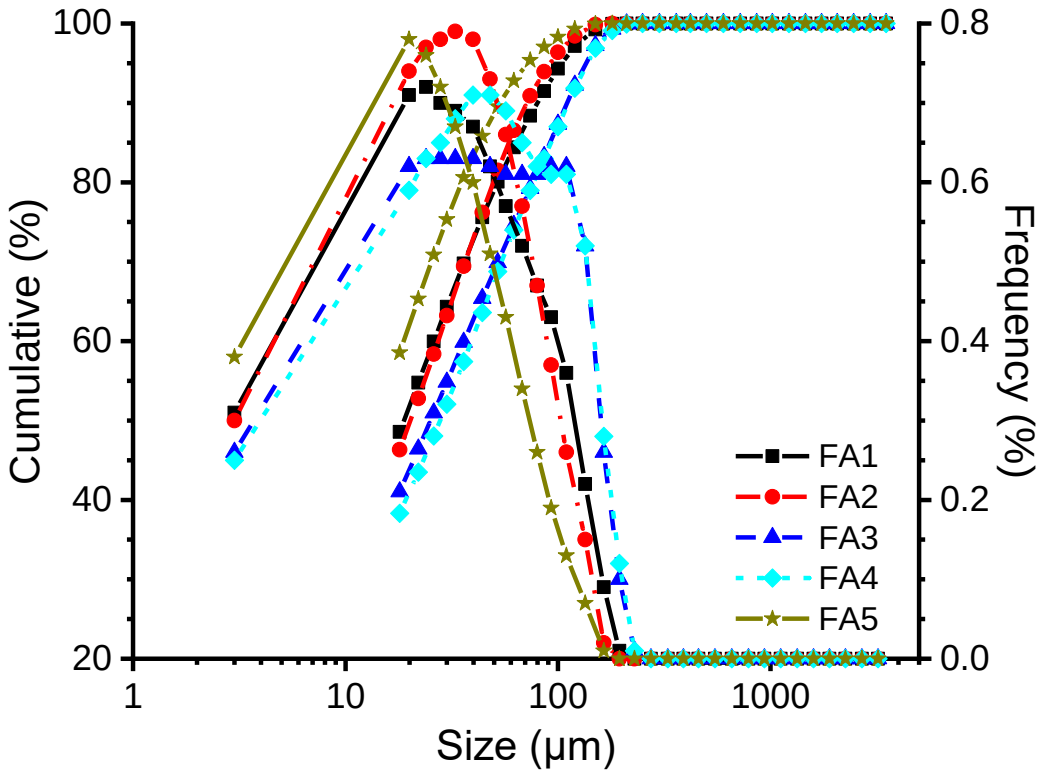

Alkali solution (by weight of the precursor)

	Na_2O	Concentration (mol/kg H_2O)	Modulus
A30	3%	2.15 (2.42)*	0
A31			1
A32			2
A50	5%	3.58 (4.03)*	0
A51			1
A52			2

$$M_s = \frac{n_{SiO_2}}{n_{Na_2O}}$$

* Alkali solution for Fly ash activation

water/slag	0.45

water/fly ash	0.40

Quantitative X-ray Diffraction (QXRD)

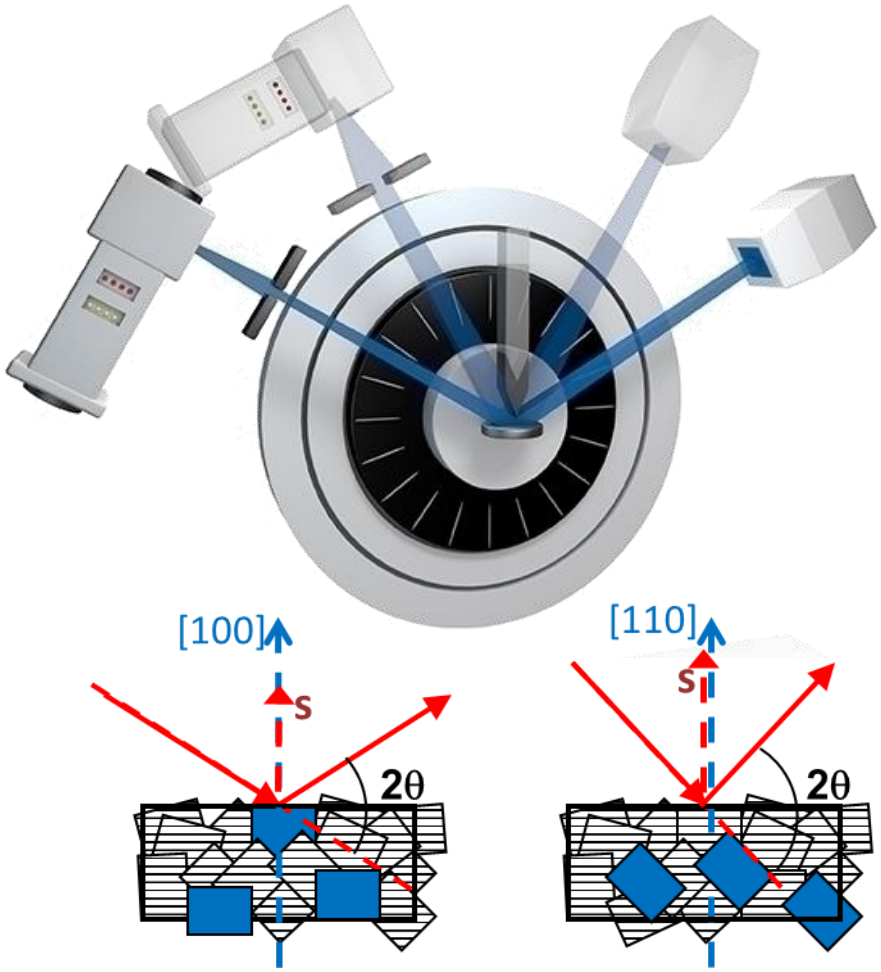

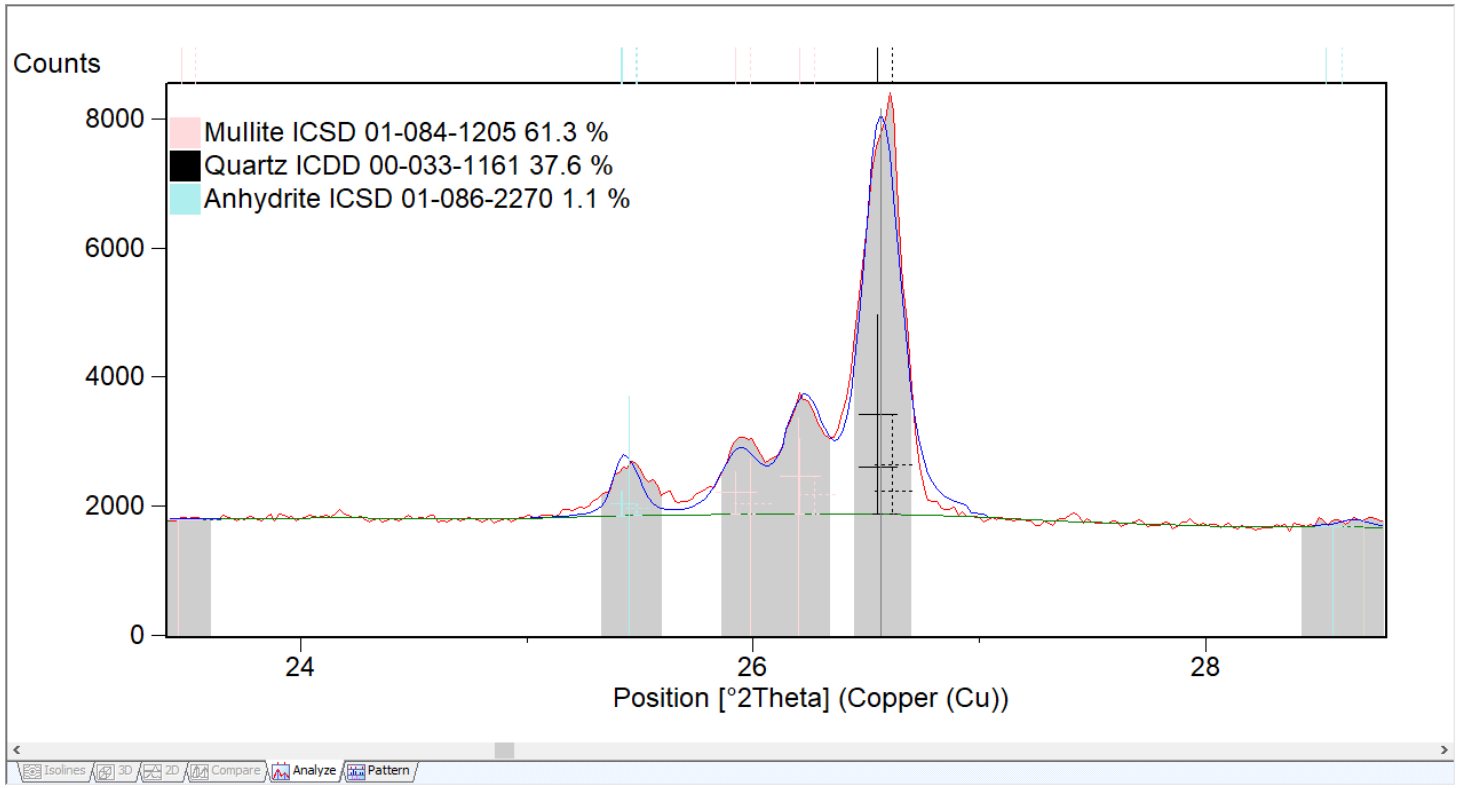

Solid state nuclear magnetic resonance (NMR)

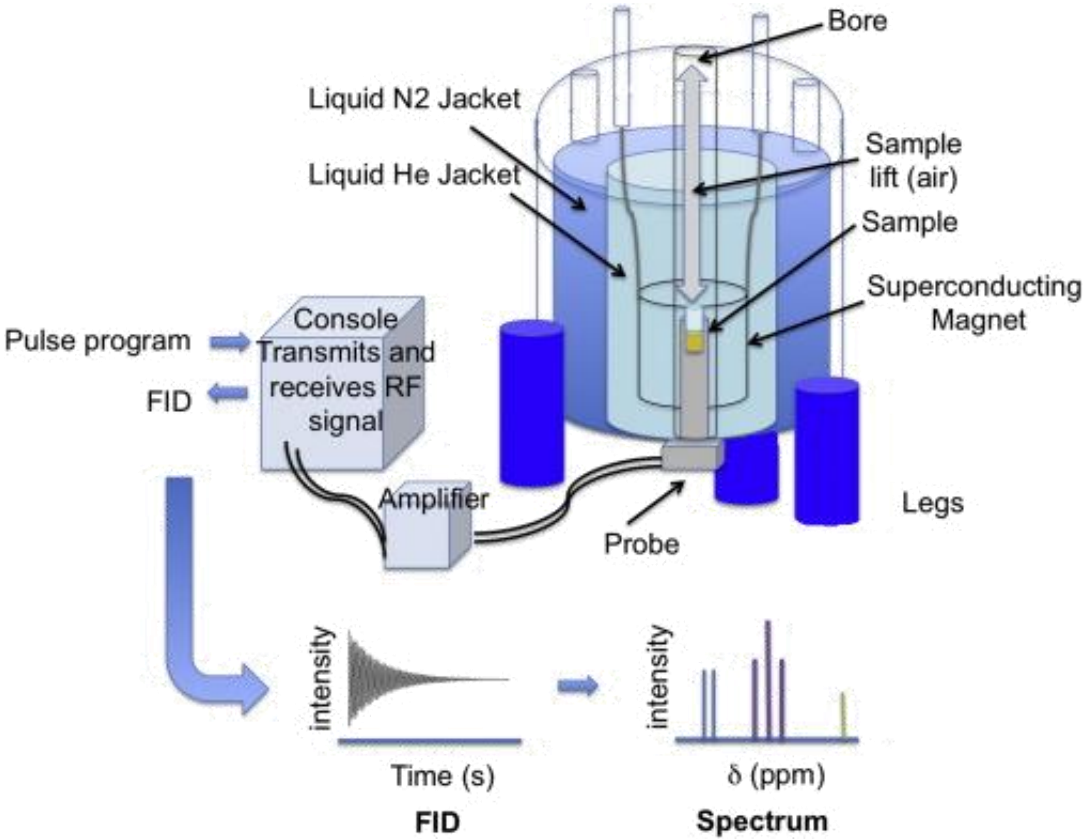

RANKIN ET AL., ATHEROSCLEROSIS. (2014)

^{29}Si

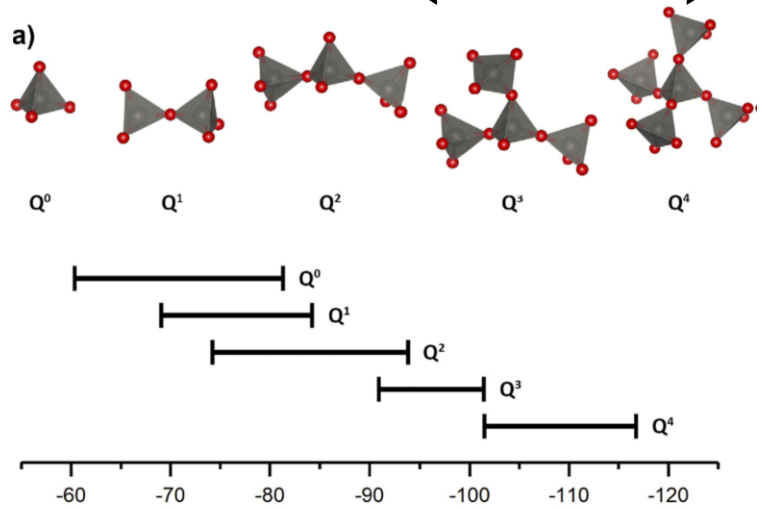

^{27}Al

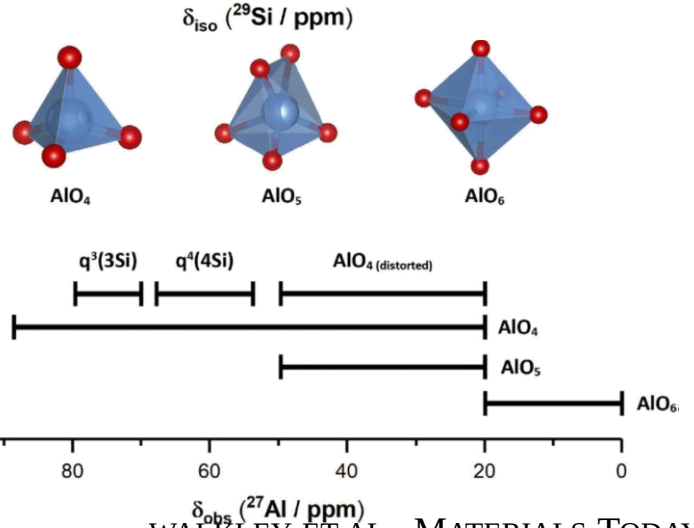

WALKLEY ET AL., MATERIALS TODAY ADVANCES. (2019)

Energy Dispersive X-ray Spectroscopy (EDX)

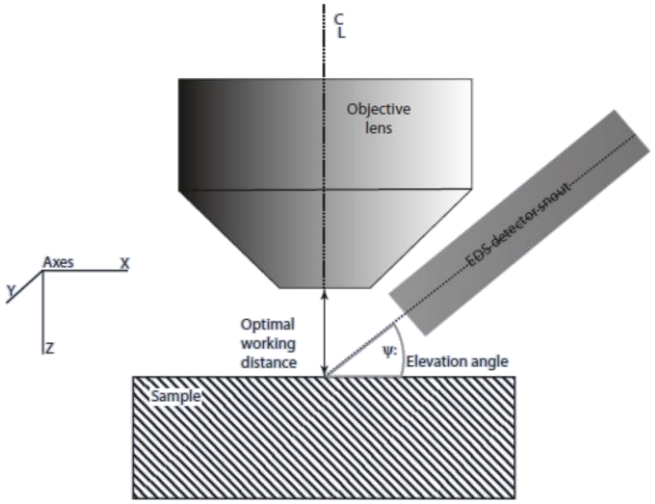

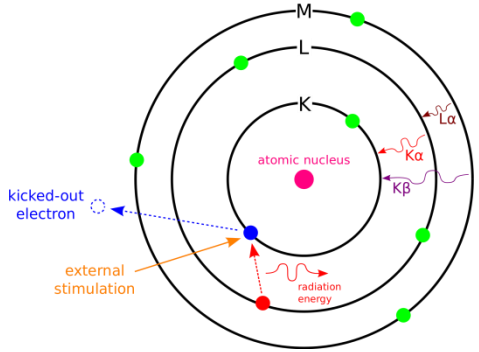

original

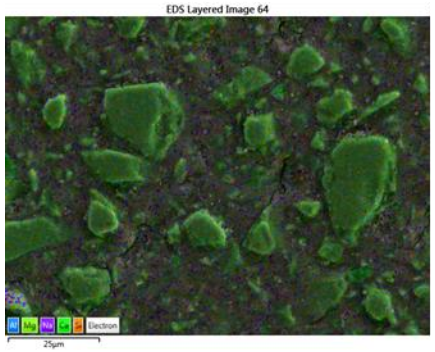

processed

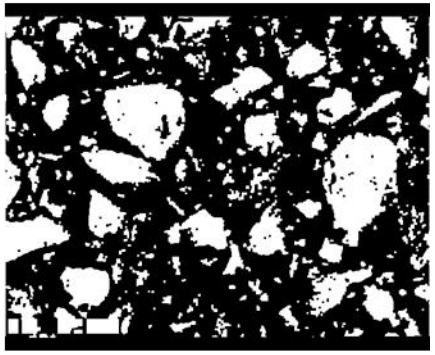

分离颜色通道

DOH by EDX-IA

侵蚀、扩张、封闭

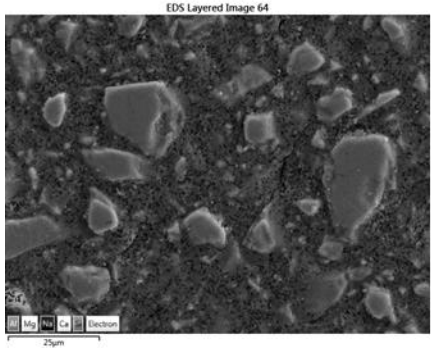

二元化处理

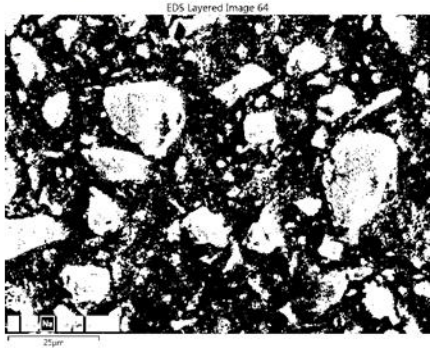

GOLDSTEIN ET AL., SCANNING ELECTRON MICROSCOPY AND X-RAY MICROANALYSIS. (2017)

Isothermal calorimetry

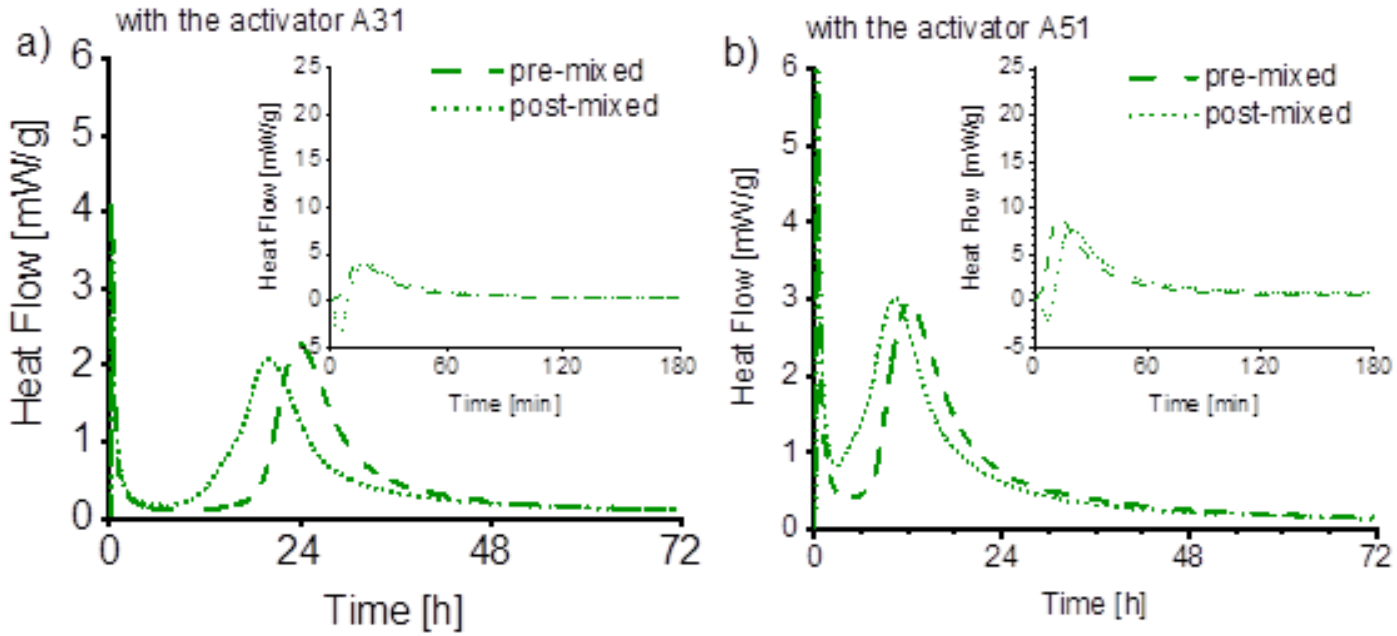

CONTENTS

1 Background

2 Methods

3 Results

4 Conclusions

Spatial distribution of main elements in the slags

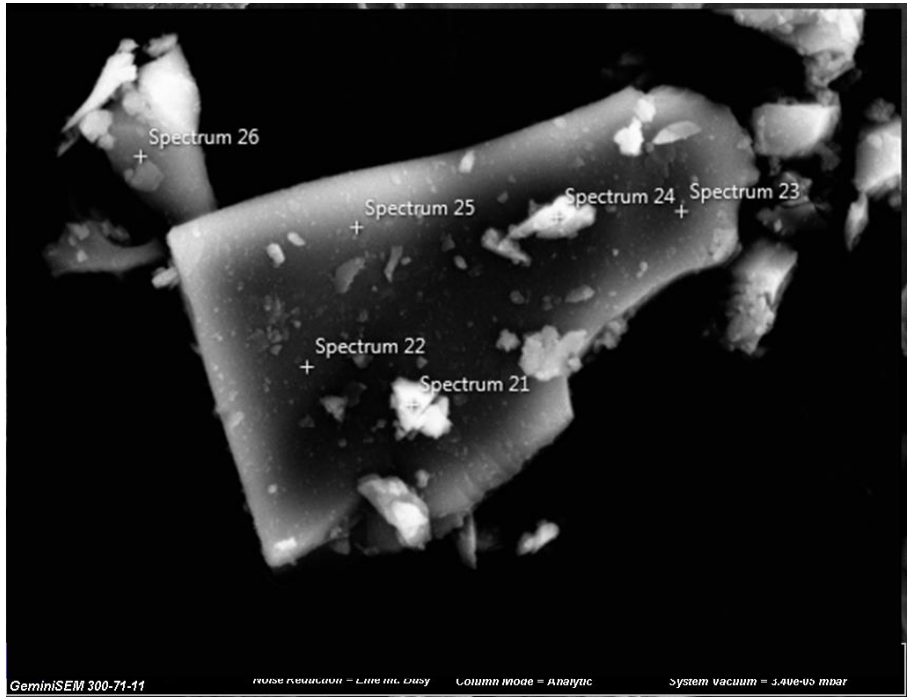

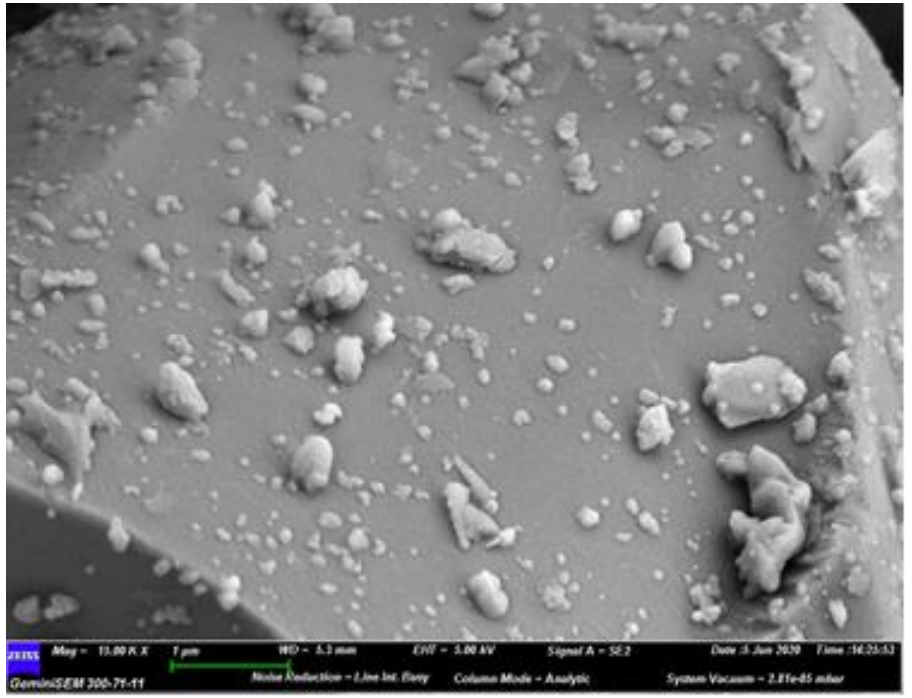

S1	SiO_2	Al_2O_3	CaO	MgO
EDX	**30.9±2.9**	**15.0±2.0**	**40.1±6.6**	**9.2±1.8**
XRF	**28.4**	**15.4**	**40.2**	**9.93**

S2	SiO_2	Al_2O_3	CaO	MgO
EDX	**34.3±1.3**	**14.6±0.9**	**41.3±2.5**	**6.4±0.8**
XRF	**31.9**	**14.5**	**42.8**	**6.71**

Si(Q^n(mAl) model applied on the slags

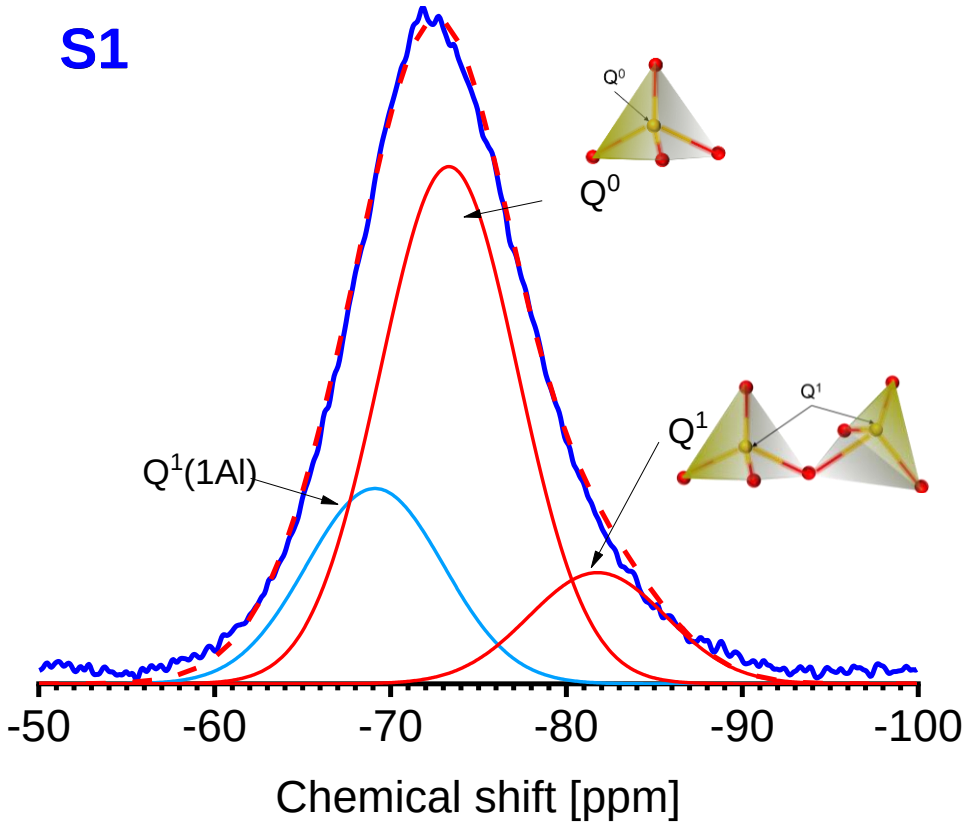

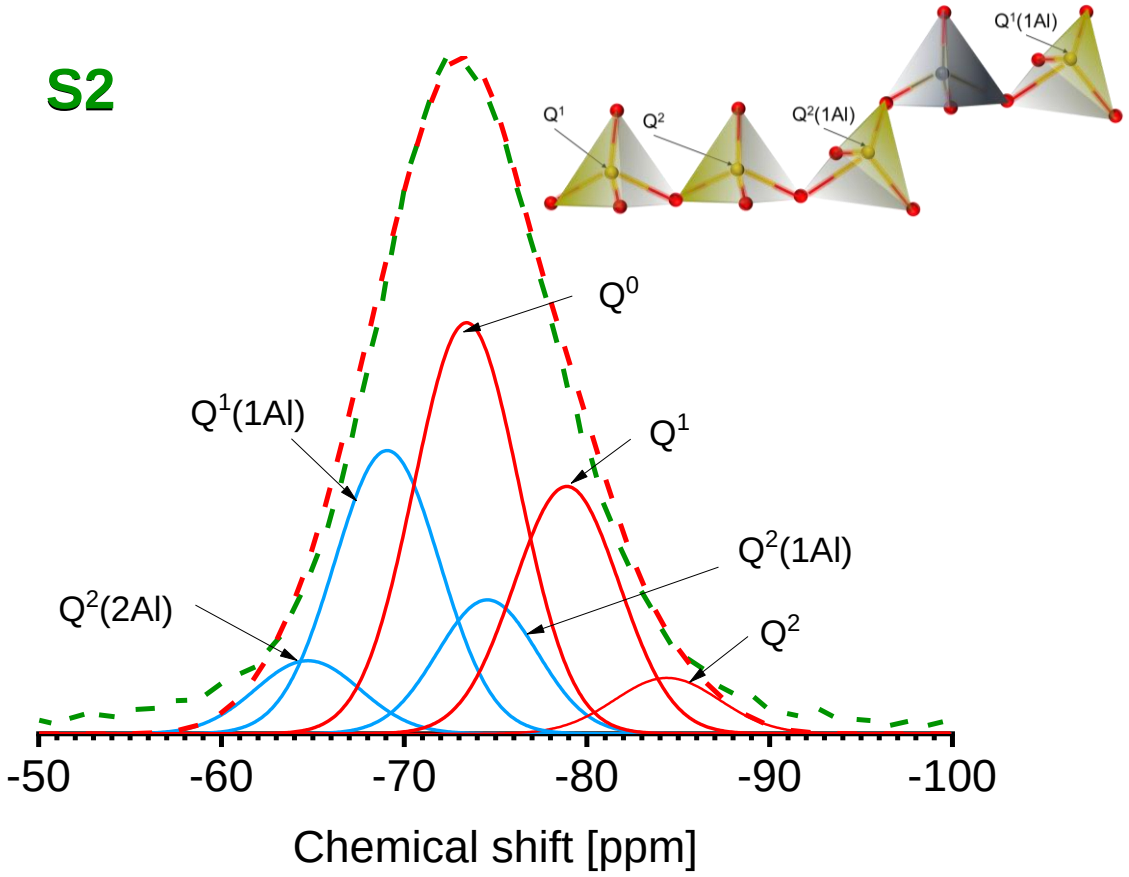

JIN ET AL., CCR. (2019)

Chemical composition of the glass phase in the fly ashes

Major crystalline phases and quartz and mullite ($Al_2(Al_{2+2x} \cdot Si_{2-2x})O_{10-x}$, x = 0.25~0.40)

	SiO_2	Al_2O_3	Fe_2O_3	TiO_2	CaO	MgO	K_2O	Na_2O	SO_3	Si/Al	M/(Fe+Al)	玻璃体含量
FA1	**51.6**	**16.3**	**6.6**	0.9	**17.2**	**4.3**	0.9	0.0	2.0	1.58	0.89	76.5
FA2	**54.0**	**13.5**	**8.7**	0.9	**15.0**	**3.5**	1.2	2.0	1.1	2.00	0.93	72.1
FA3	**65.7**	**10.6**	**7.6**	1.6	**8.1**	**3.9**	1.1	1.2	0.2	3.11	0.78	56.7
FA4	**66.3**	**17.2**	**5.1**	1.3	**4.5**	**2.8**	1.3	0.8	0.8	1.93	0.38	66.1
FA5	**43.9**	**11.6**	**11.8**	0.7	**19.7**	**7.7**	1.2	1.9	1.4	1.89	1.24	84.6

Spatial distribution of main elements in the fly ashes

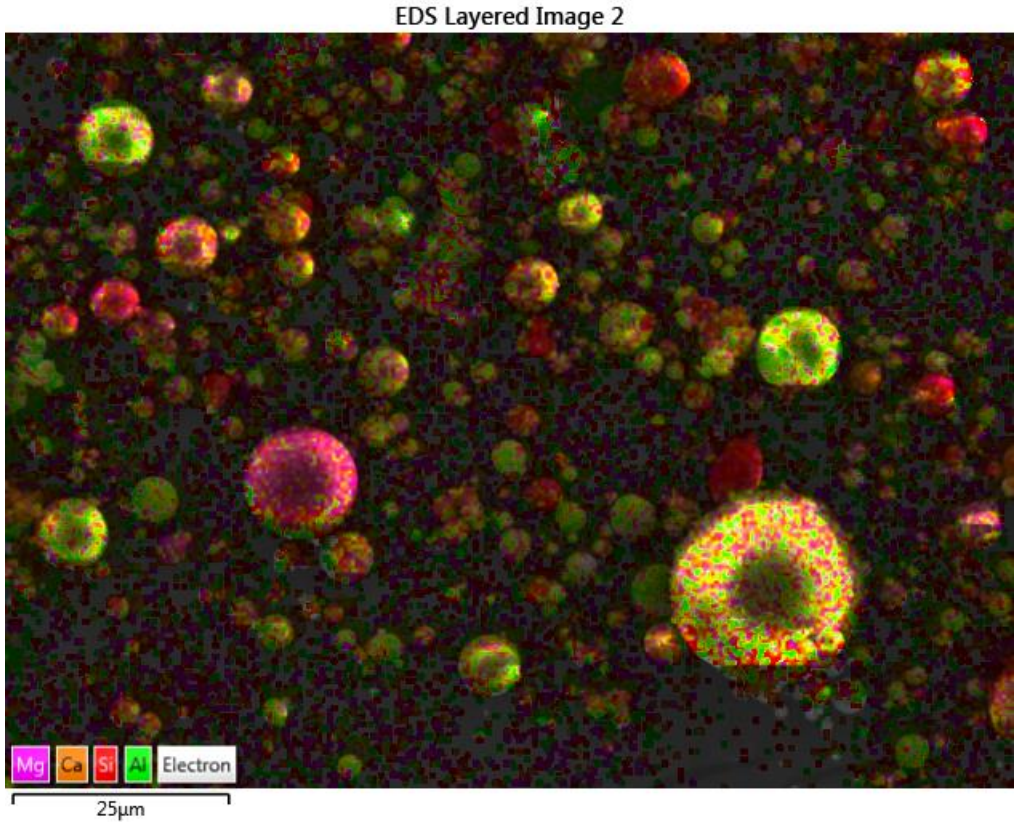

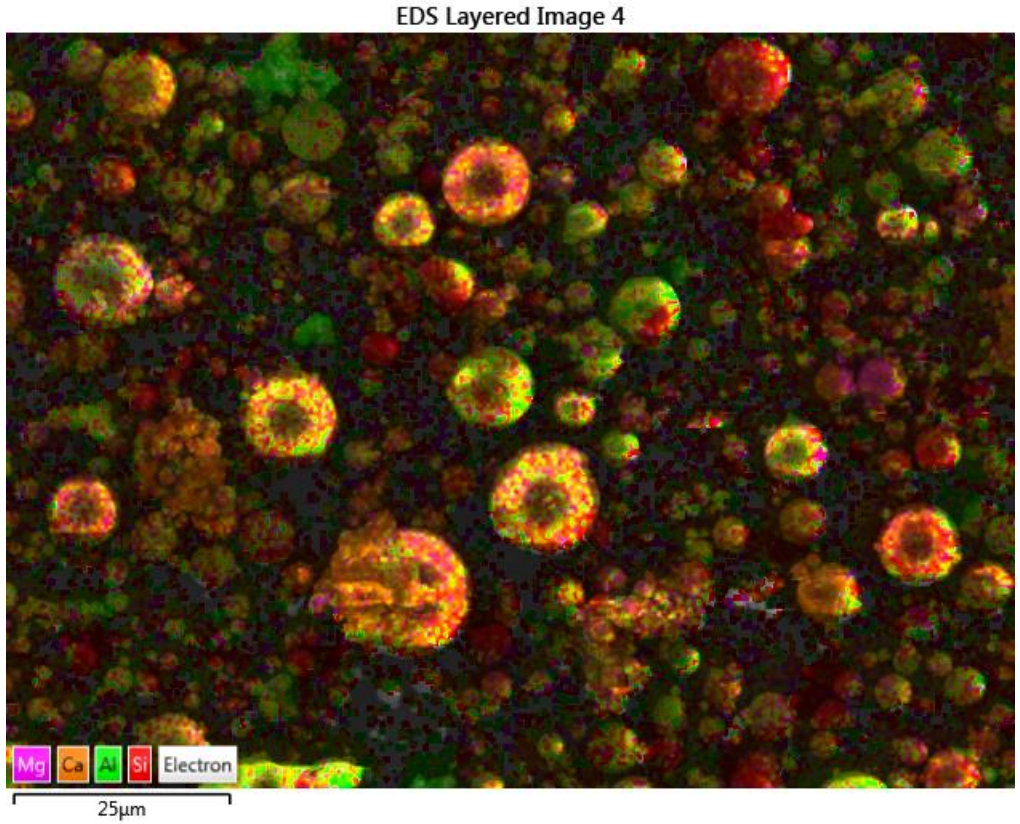

Chemical state of Al and Si in the glass phase

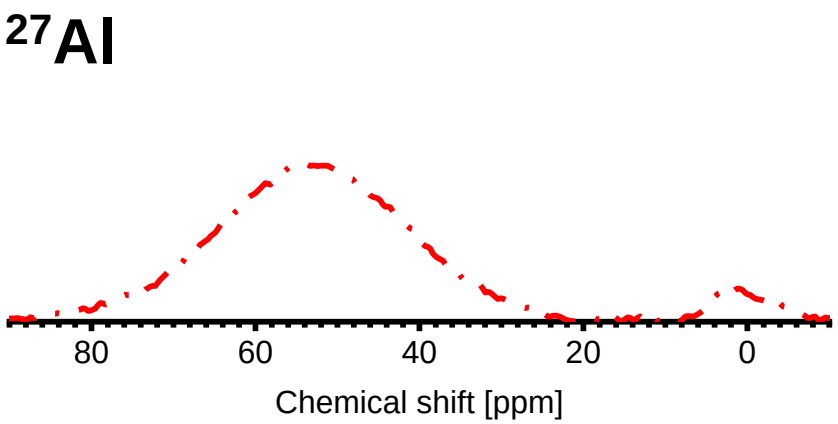

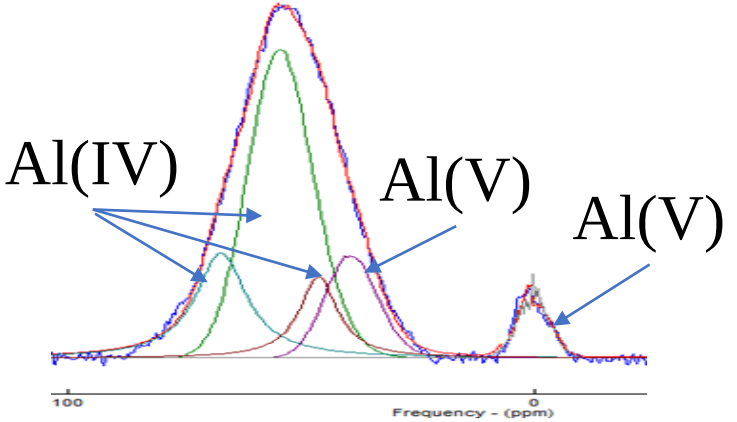

Curve fitting by Czjzek model

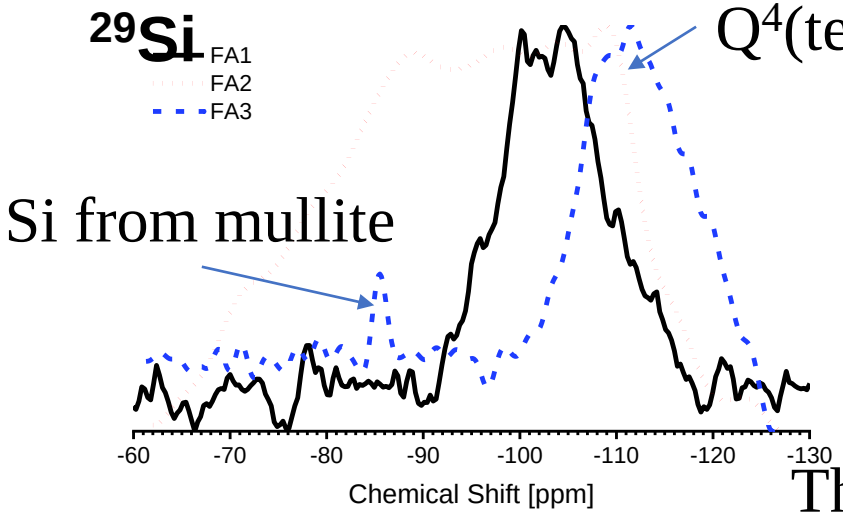

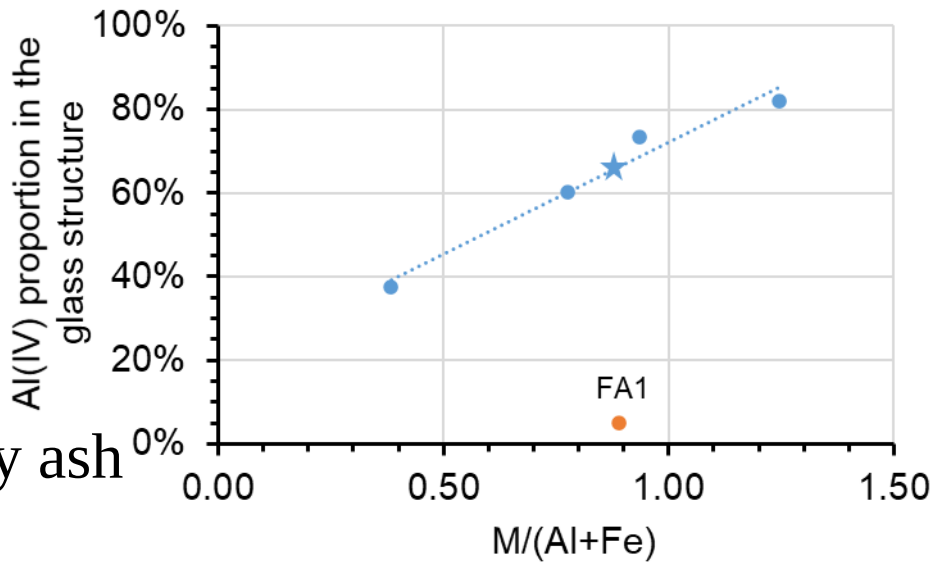

The thermal history of fly ash determines as well

The modelled glass structure in fly ash

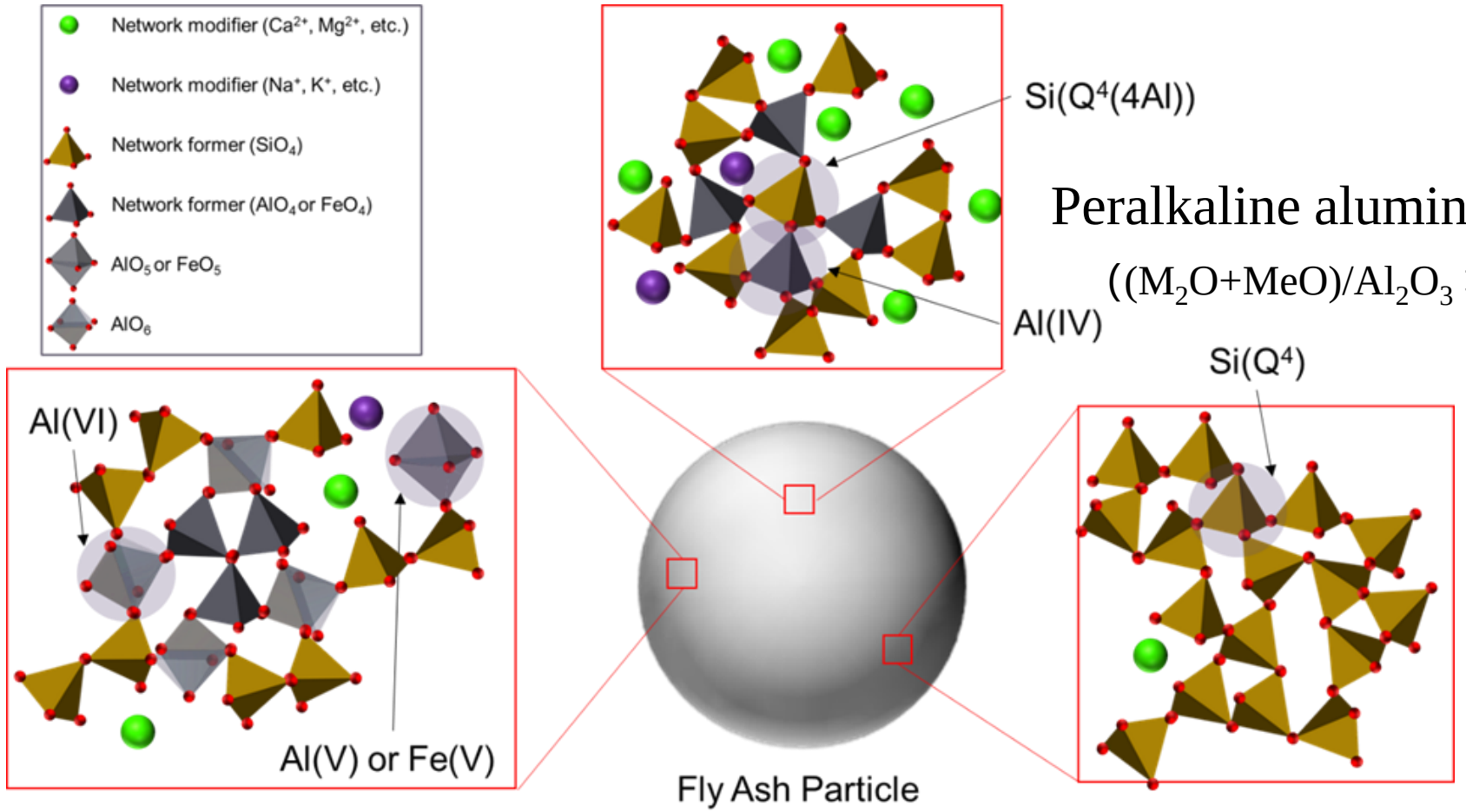

Peralkaline aluminosilicate

($(M_2O+MeO)/Al_2O_3 > 1$)

Peraluminous aluminosilicate

($(M_2O+MeO)/Al_2O_3 < 1$)

quartz

Cumulative heat VS (pseudo) **N**on-**B**ridging **O**xygen per **T**etrahedron

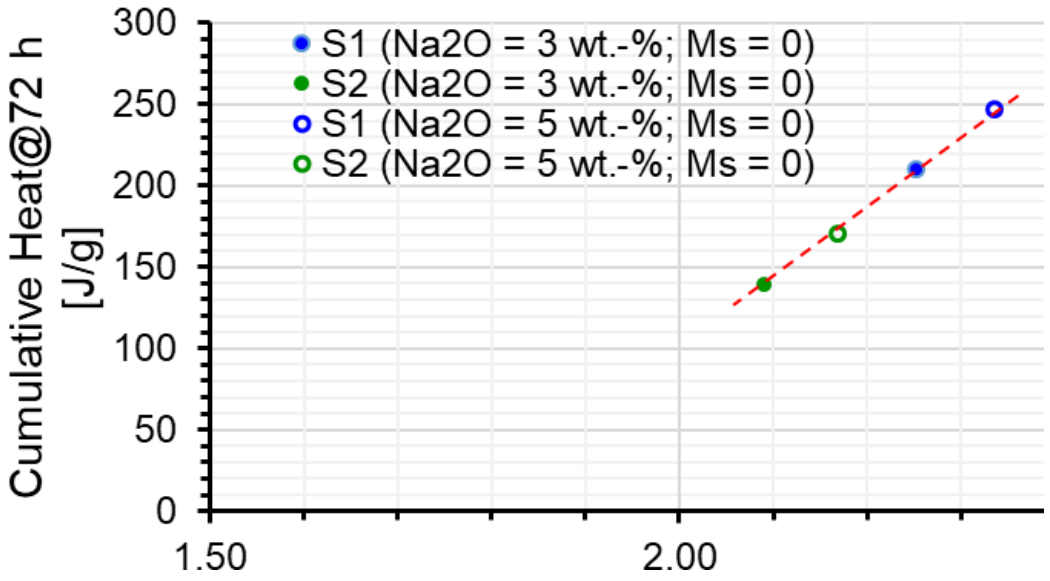

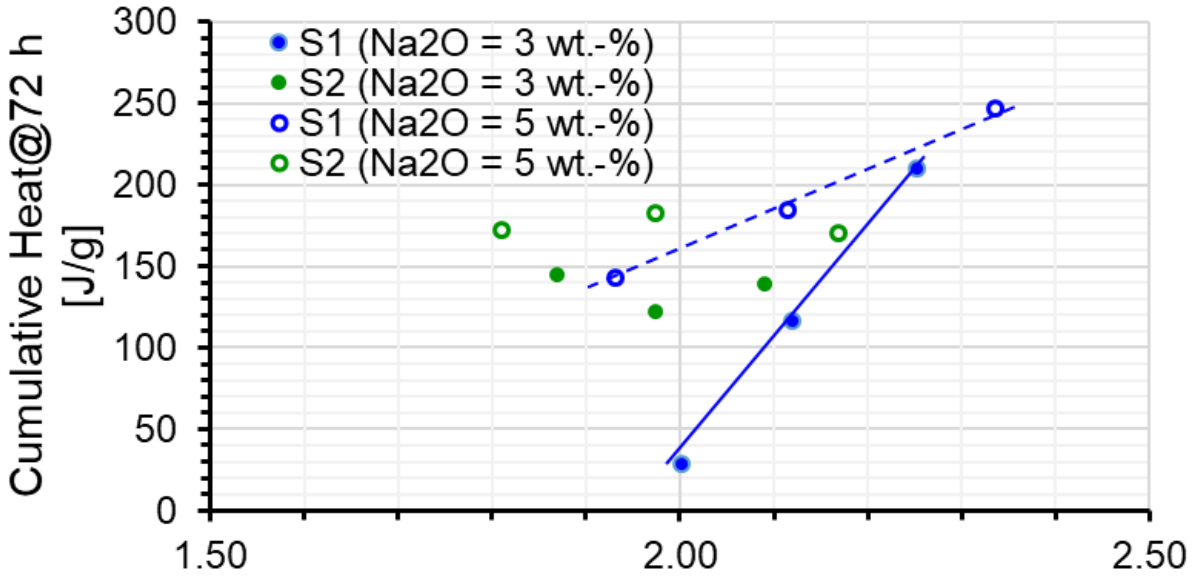

$$\frac{2 \times (X_{Ca} + X_{Mg}) + X_K + X_{Na^*} - X_{Al}}{X_{Si^*} + X_{Al}}$$

including χ_{Na} and χ_{Si} from activator

Cumulative heat VS (pseudo) **N**on-**B**ridging **O**xygen per **T**etrahedron

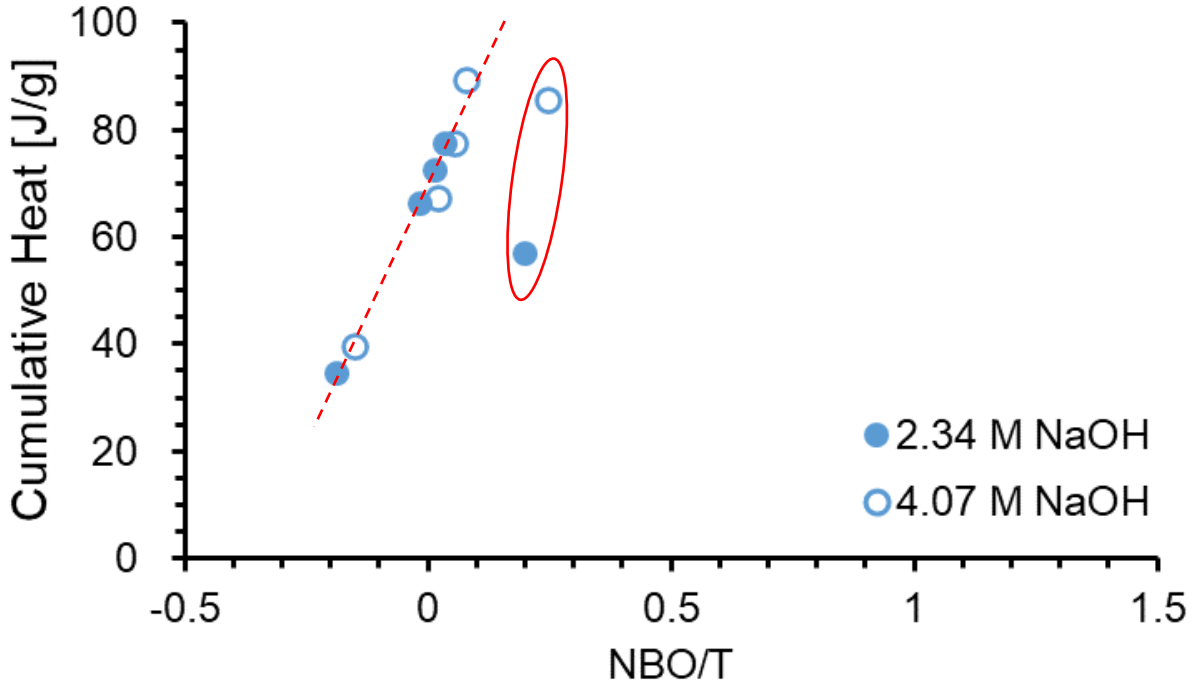

$$\frac{2*(X_{Ca} + X_{Mg}) + X_K + X_{Na} - X_{Al} - X_{Fe} - 2*X_S}{X_{Si} + X_{Al} + X_{Fe}}$$

including χ_{Na} from activator

Degree Of Hydration in the alkali activated slags

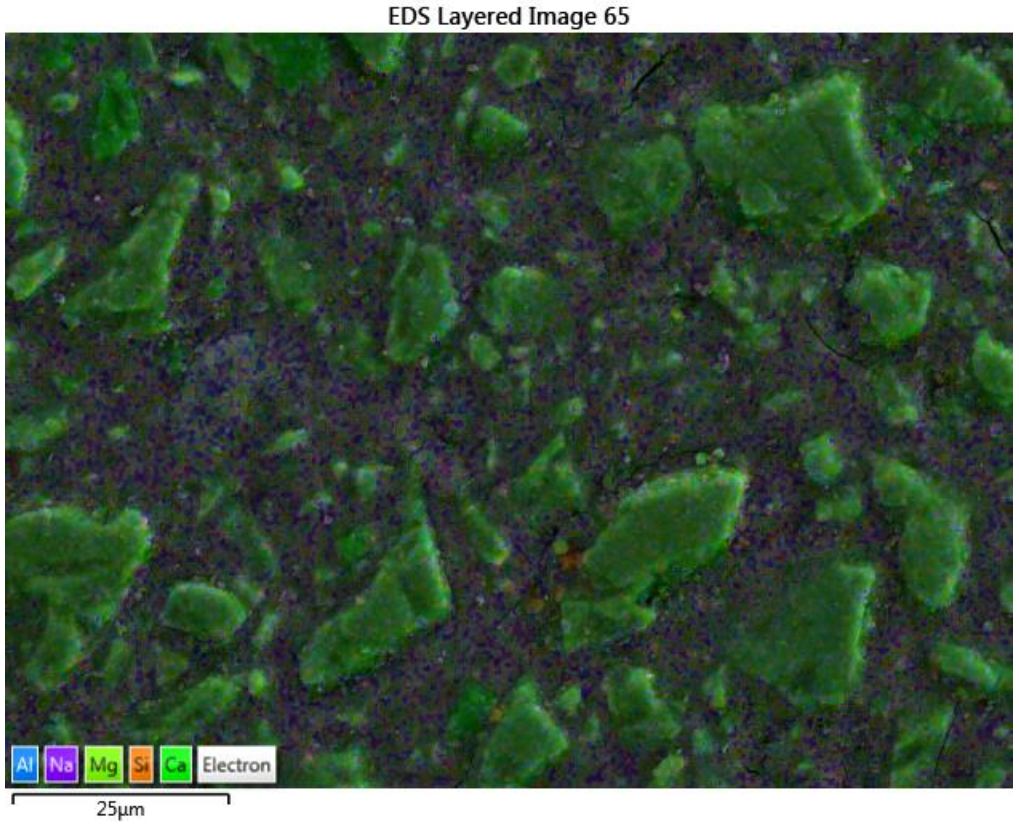

A30
A50
A31
A51
A32
A52

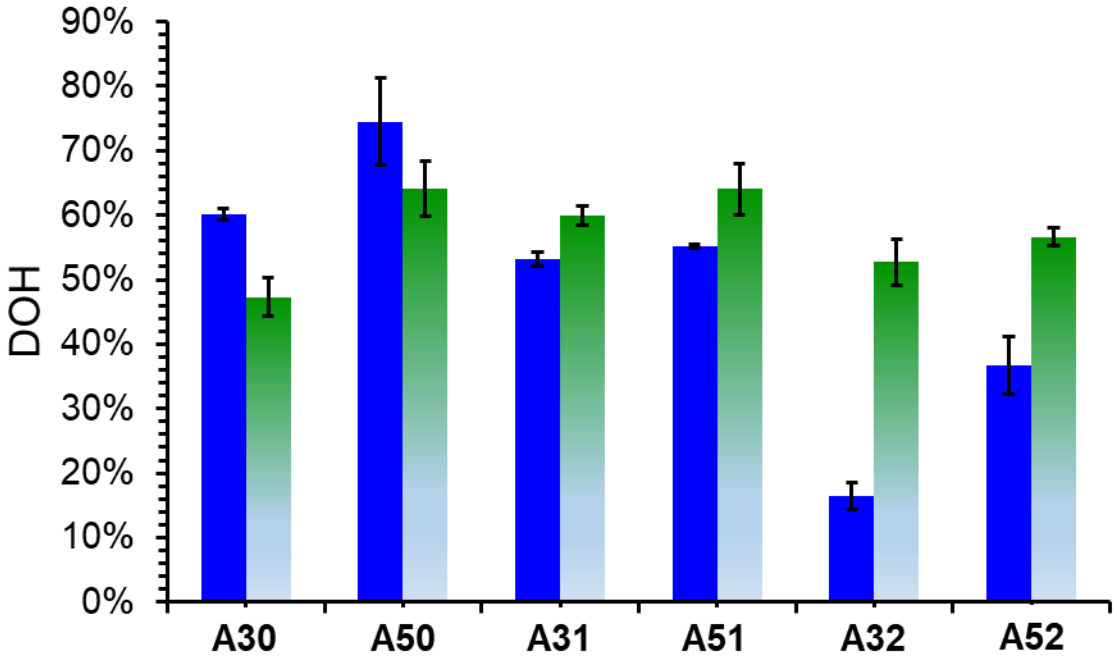

DOH VS (pseudo) **NBO/T** and cumulative heat

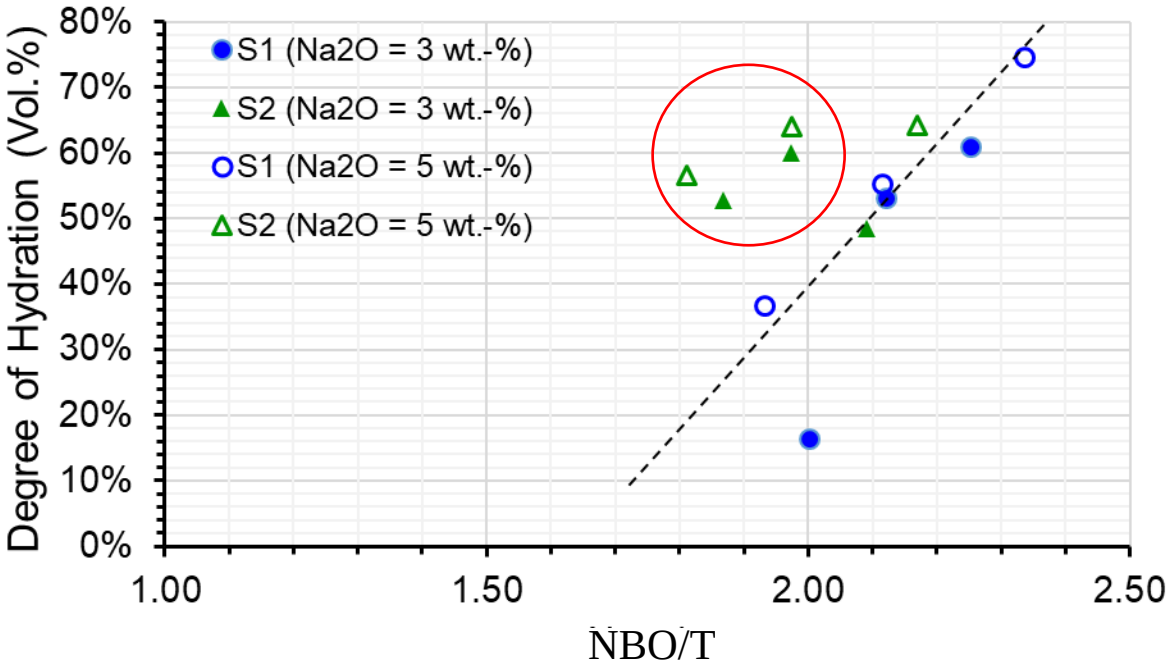

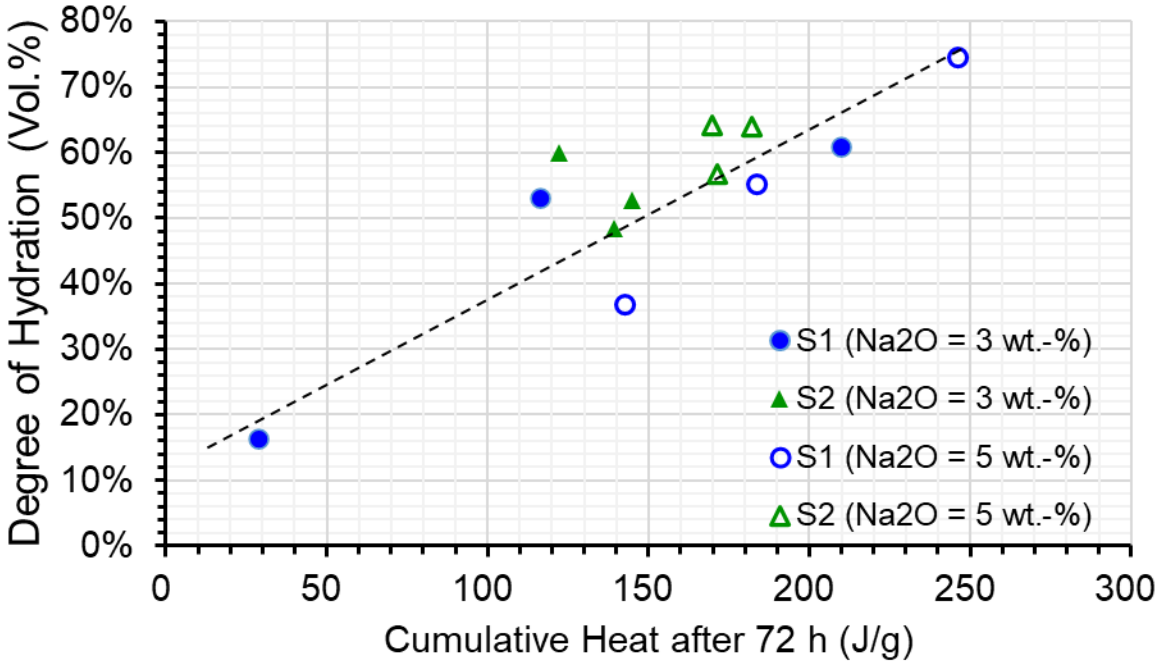

DOH of slag S2 shows low relevant to the NBO/T

Si-rich slag particles and alkali activation condition

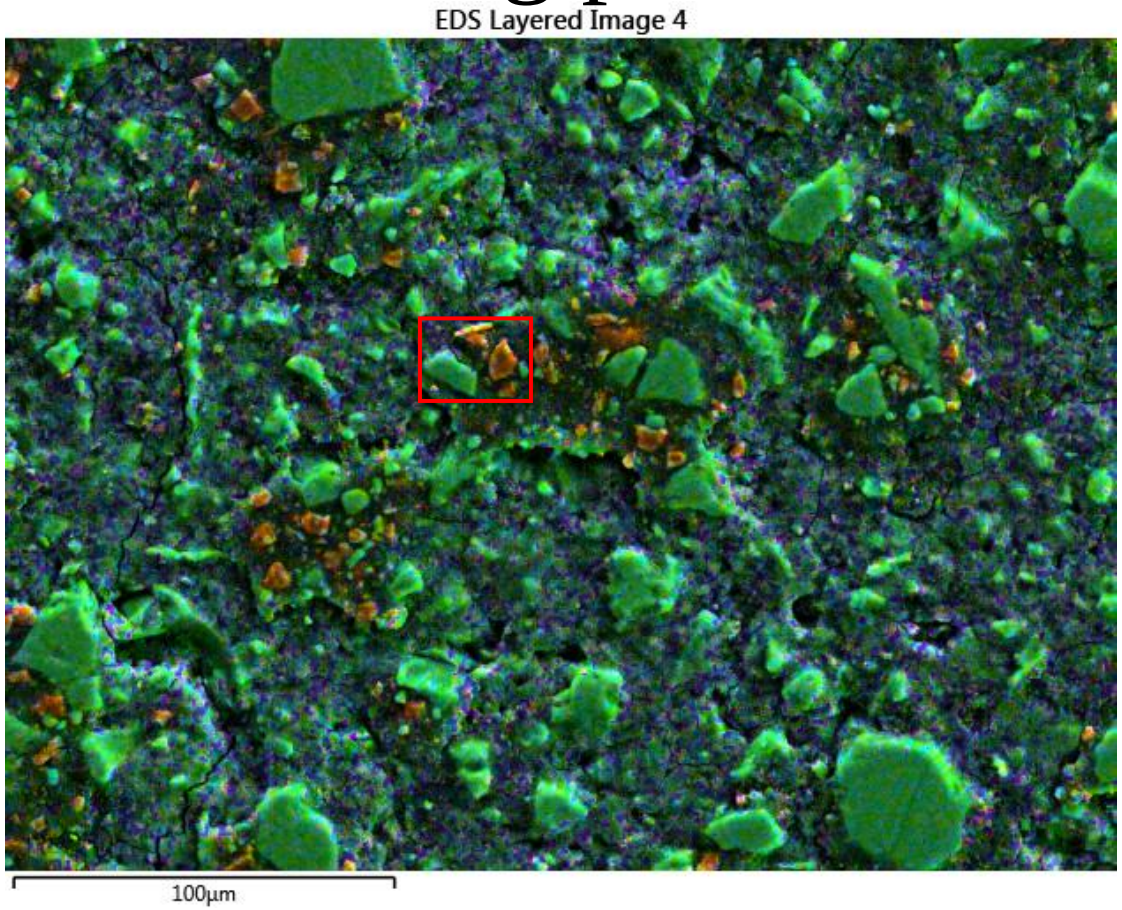

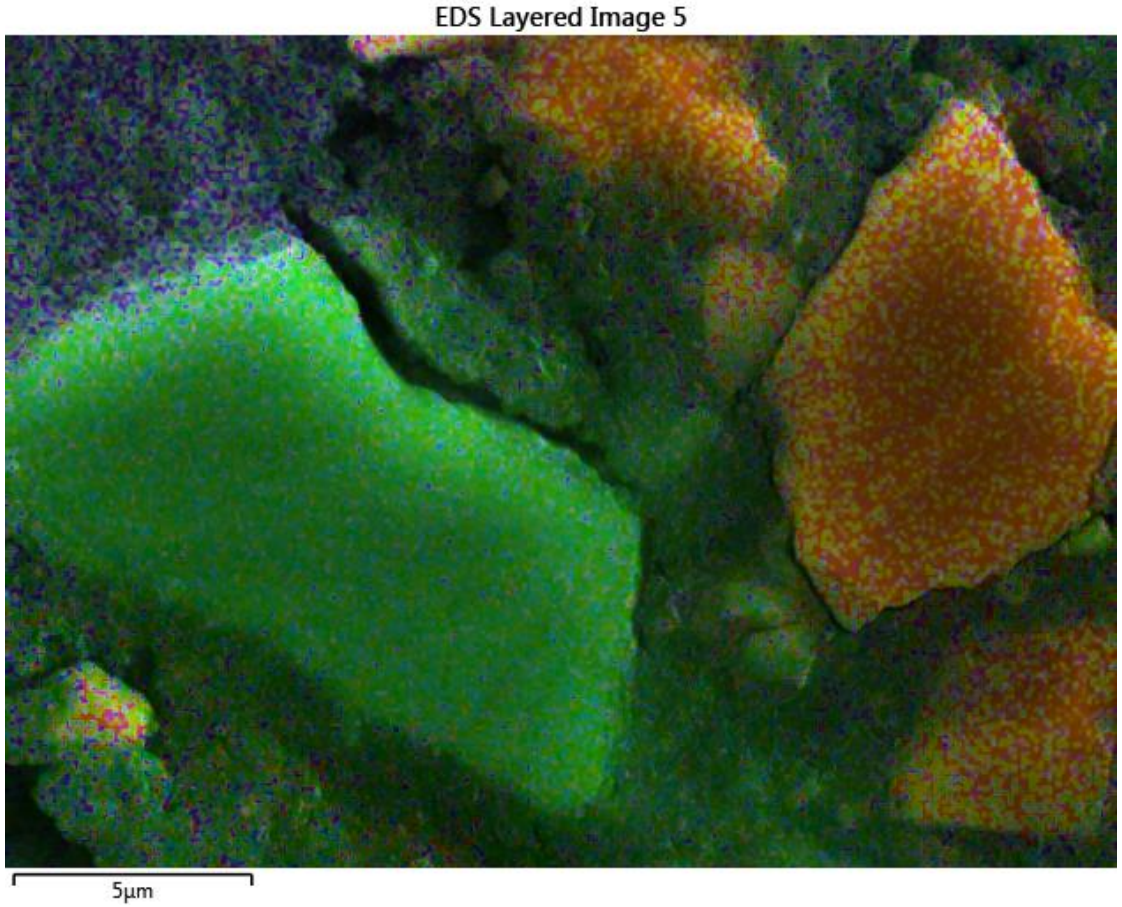

Si-rich slag particles in the hardened paste (in orange)

Morphology of Si-rich slag particles

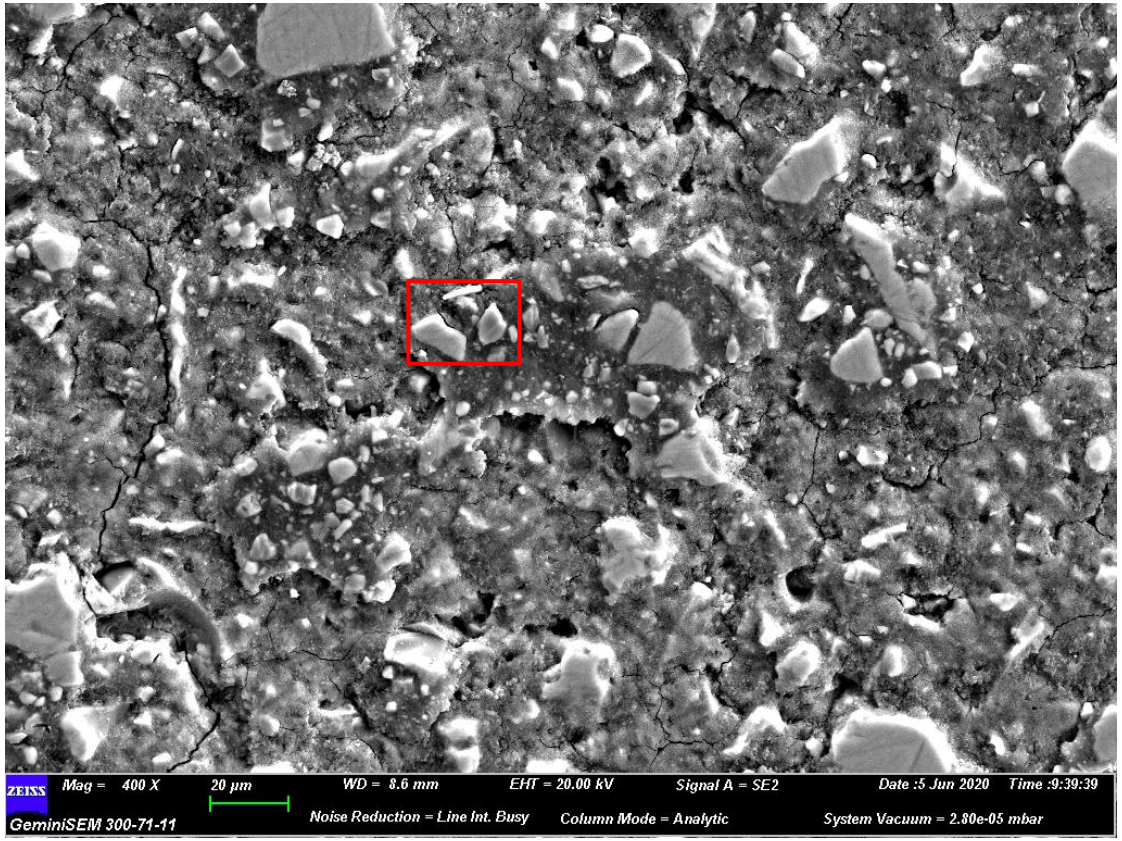

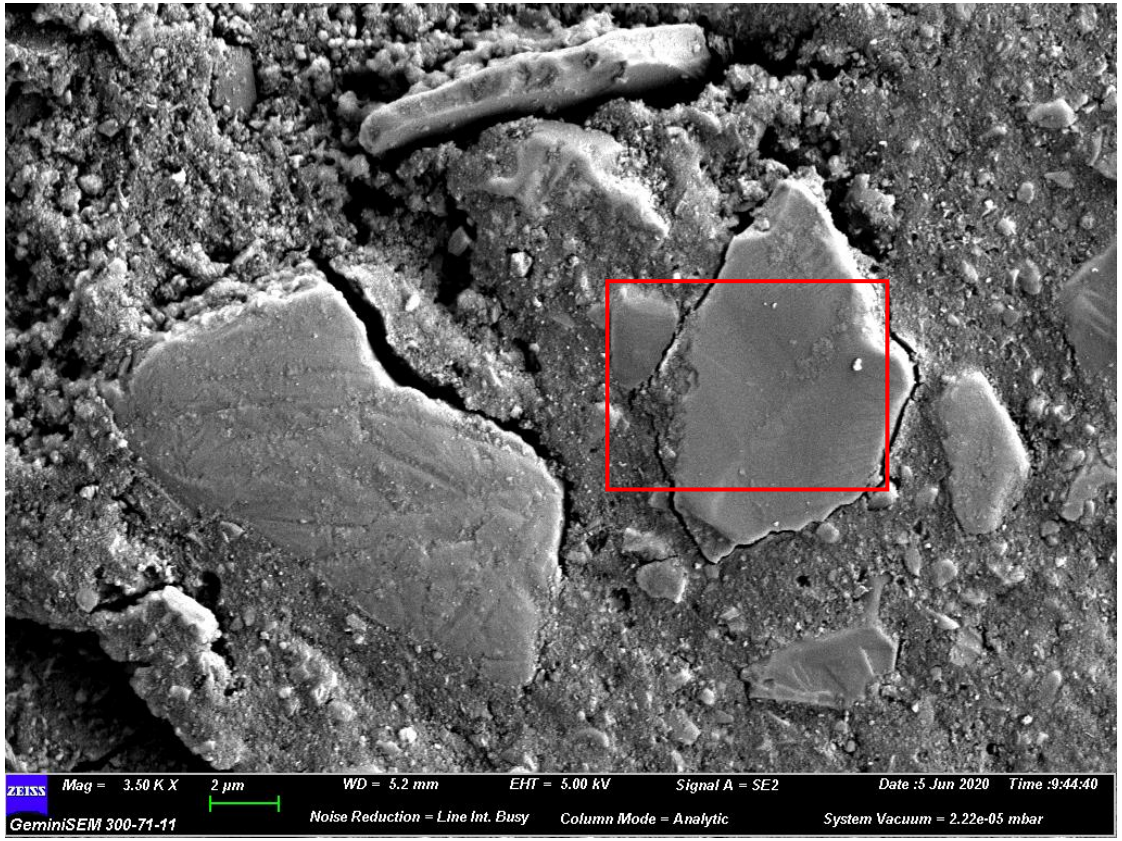

Morphology of Si-rich slag particles

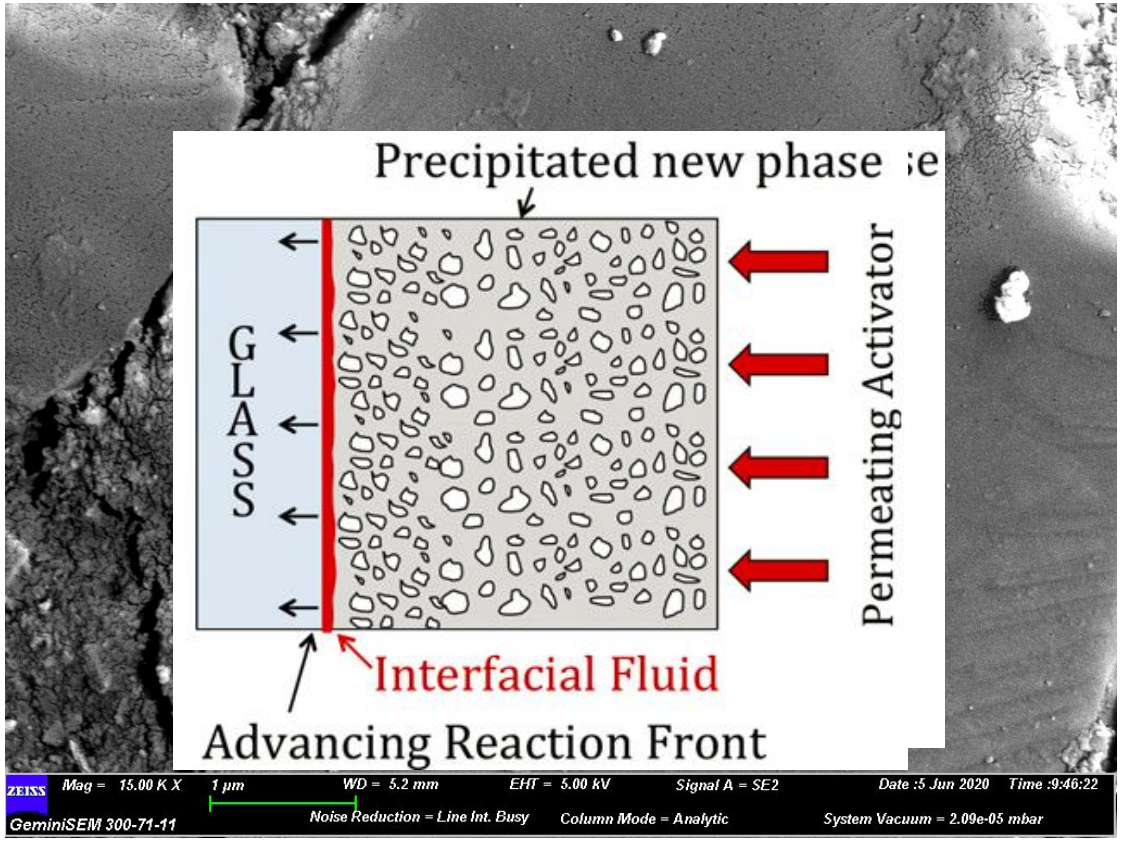

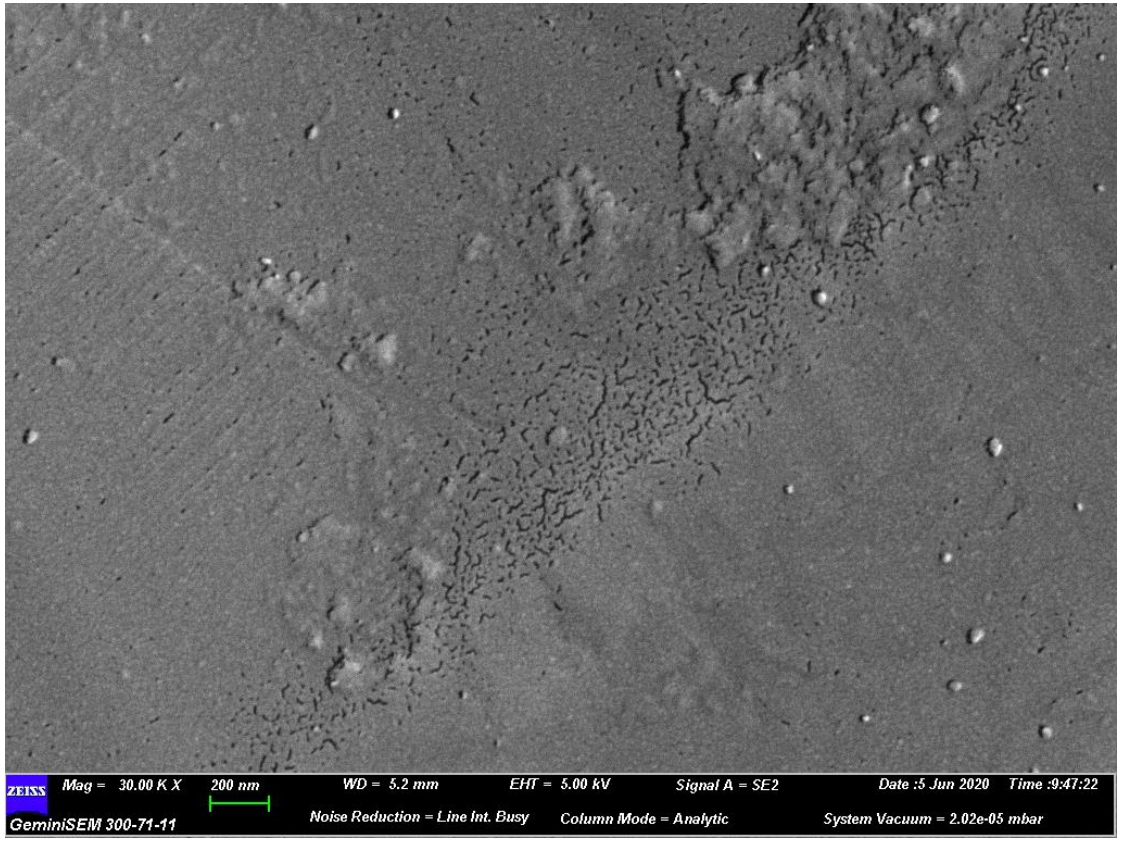

Dissolution-reprecipitation mechanism

Hydration products of alkali activated slag

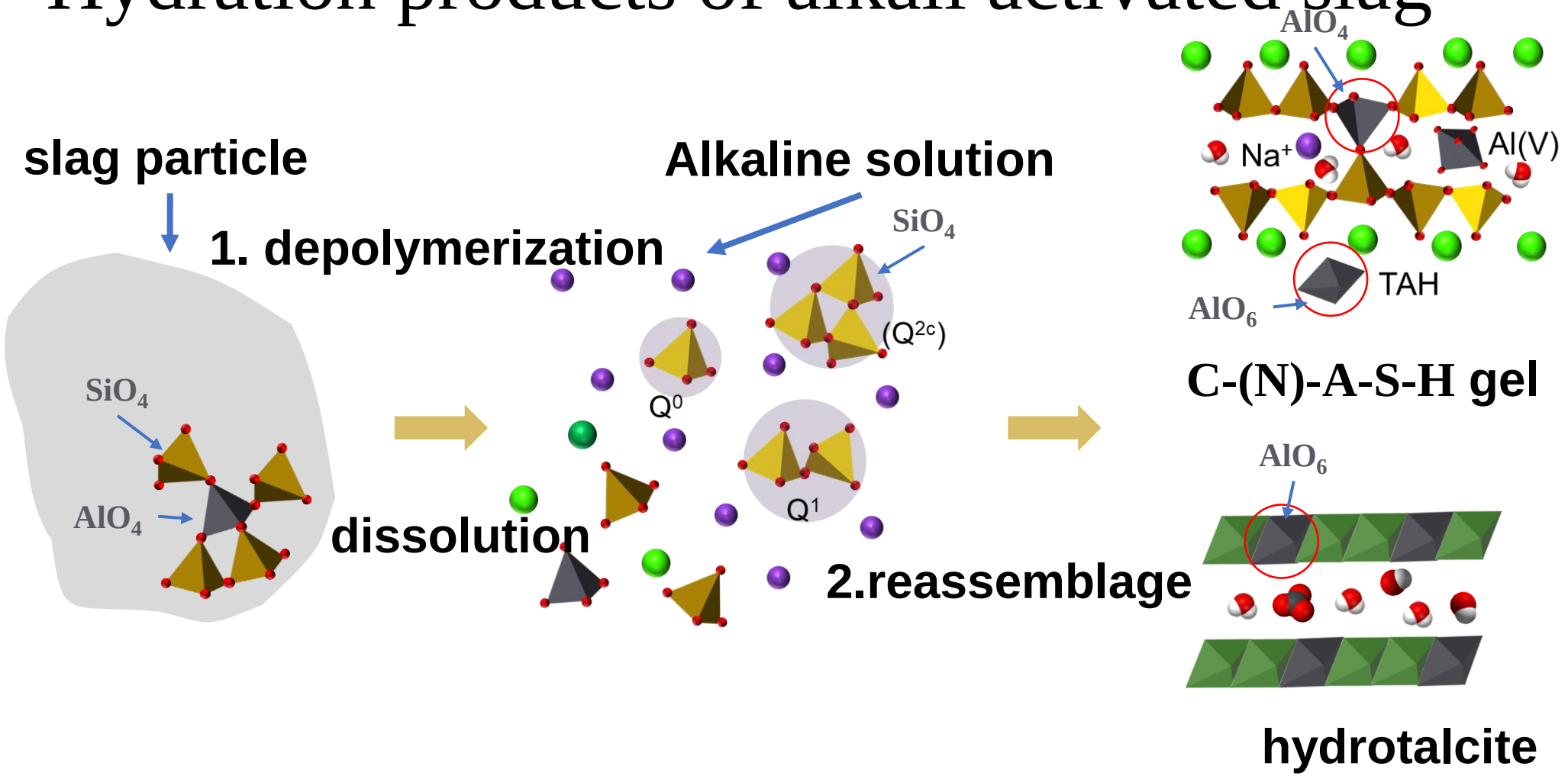

Chemical composition of the AAS paste

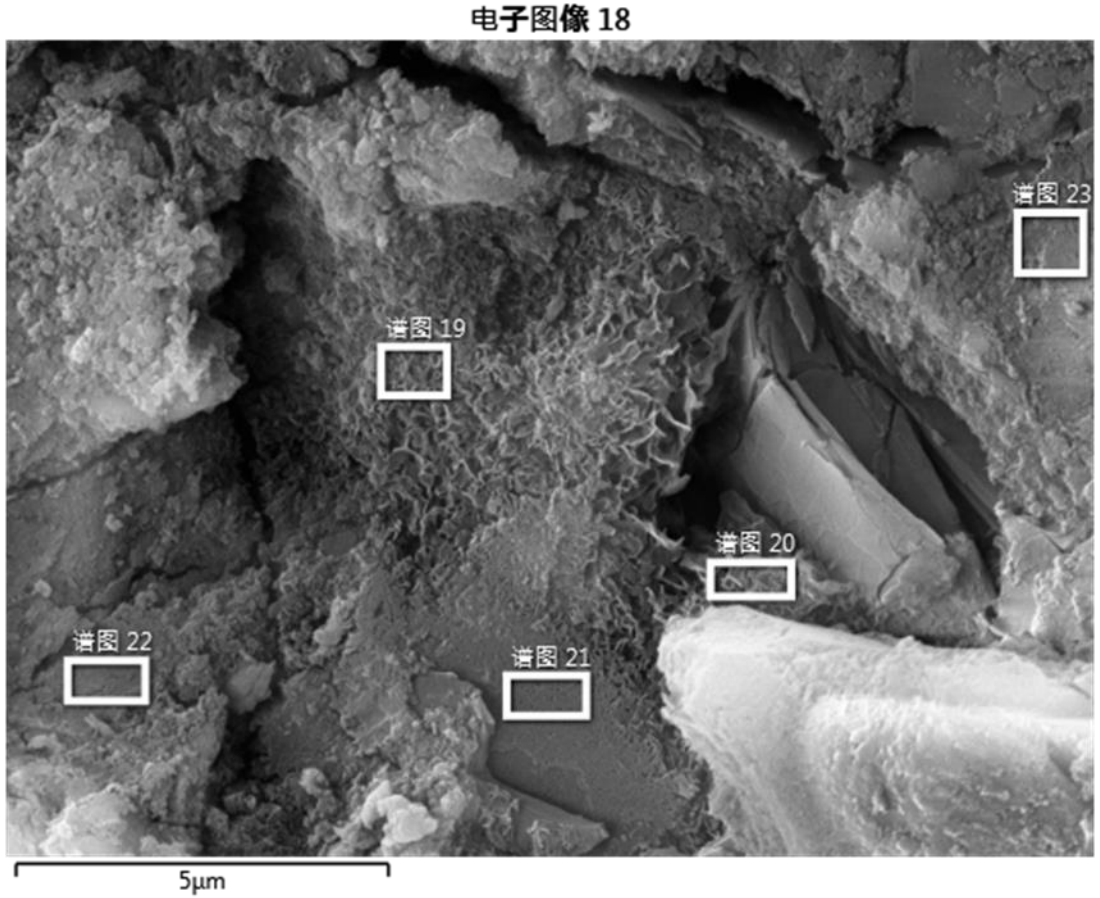

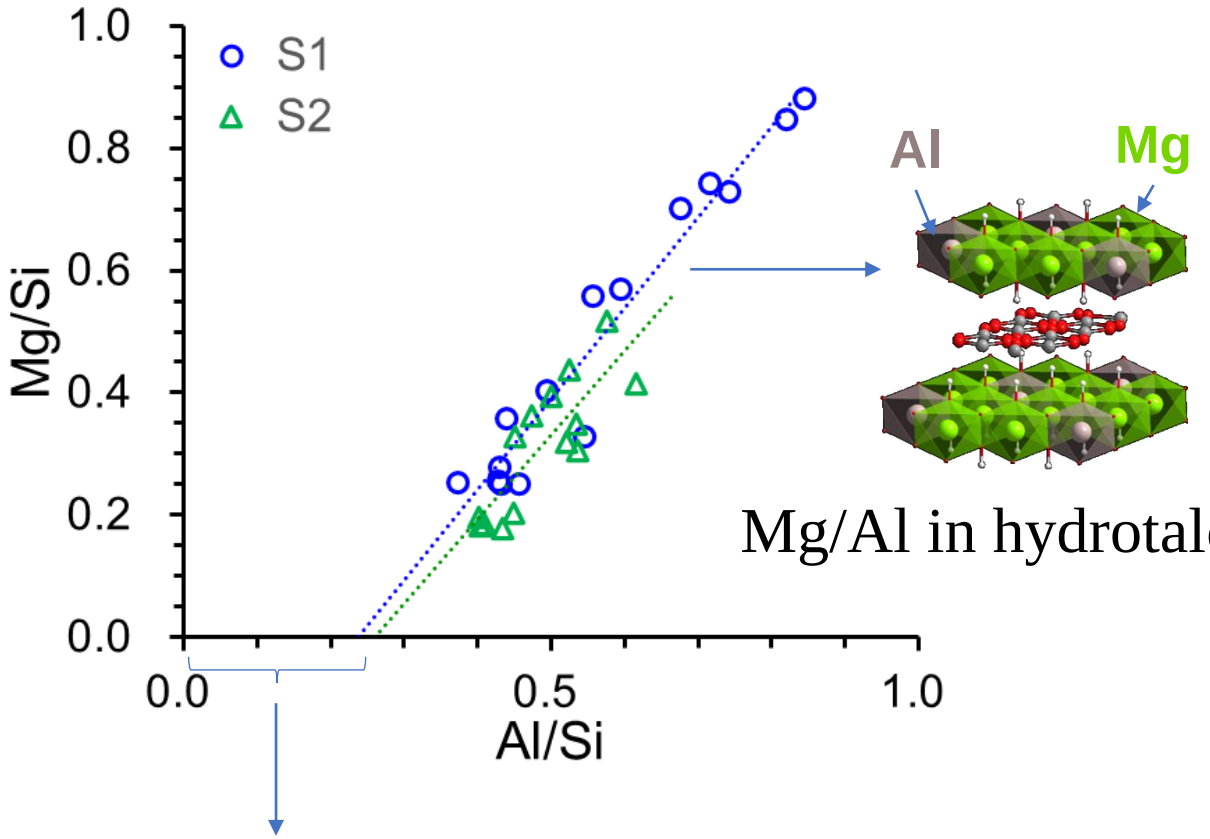

Mg/Al in hydrotalcite

Al/Si in C-(N)-A-S-H gel

Chemical composition of the AAS paste

Mg/Al in hydrotalcite ranges from 2~5

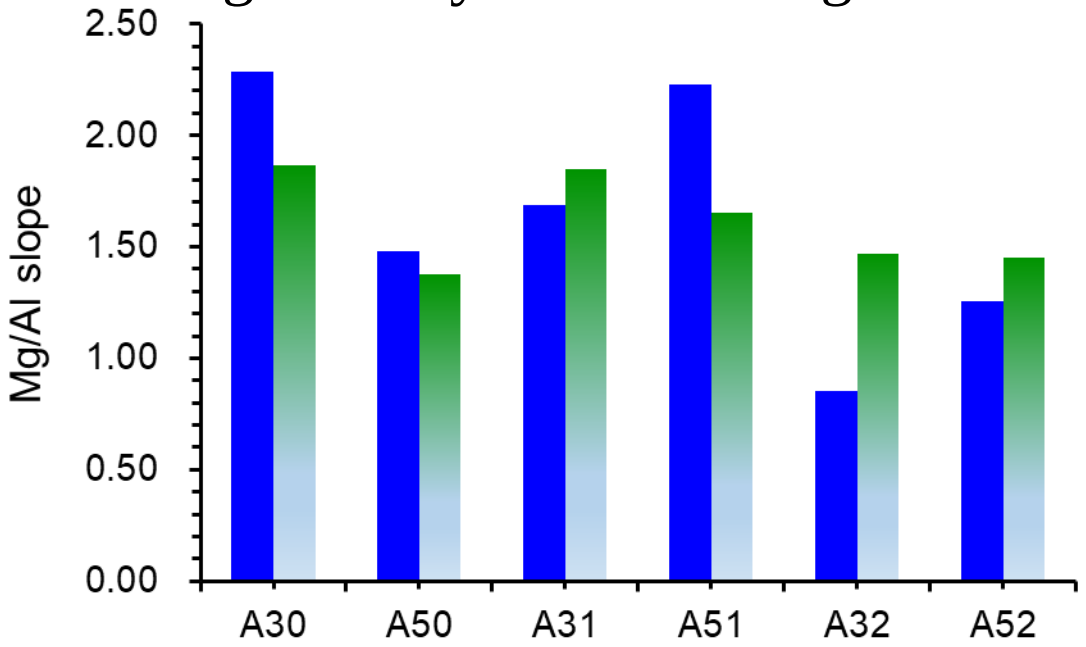

Al/Si in C-A-S-H gel limited to 0.19

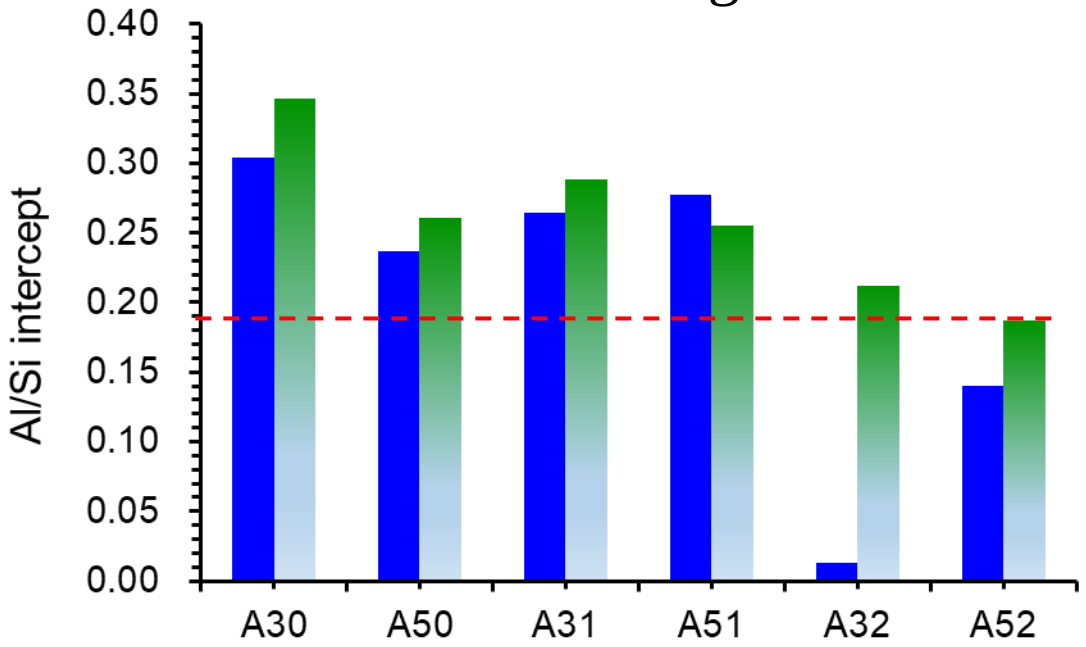

hydrotalcite intermixed with C-A-S-H gel

Al(VI) ratio in the pastes

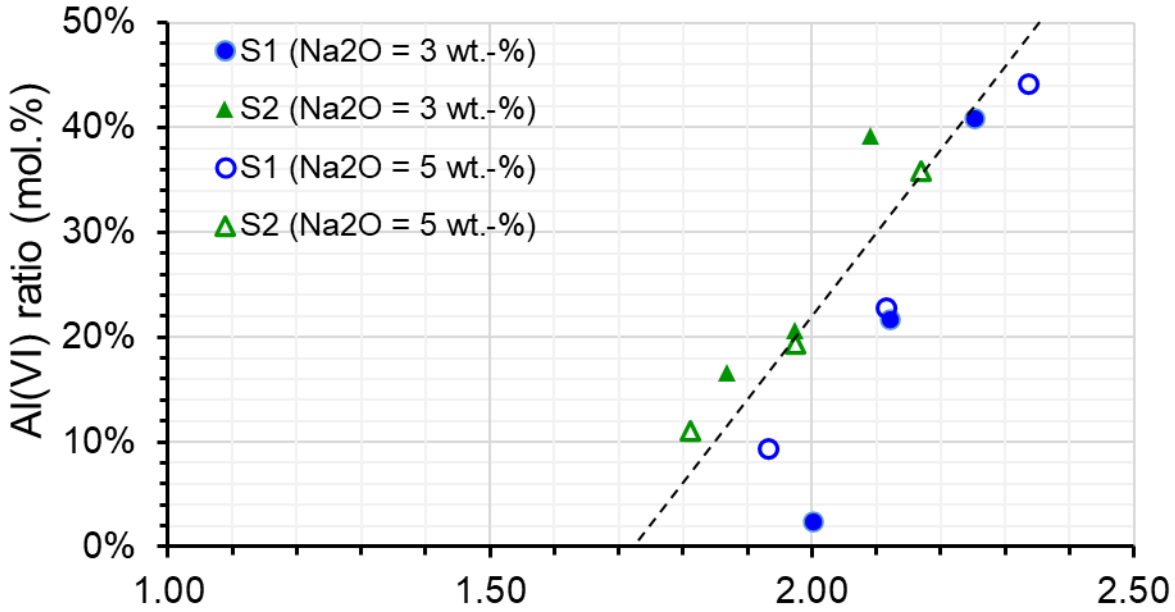

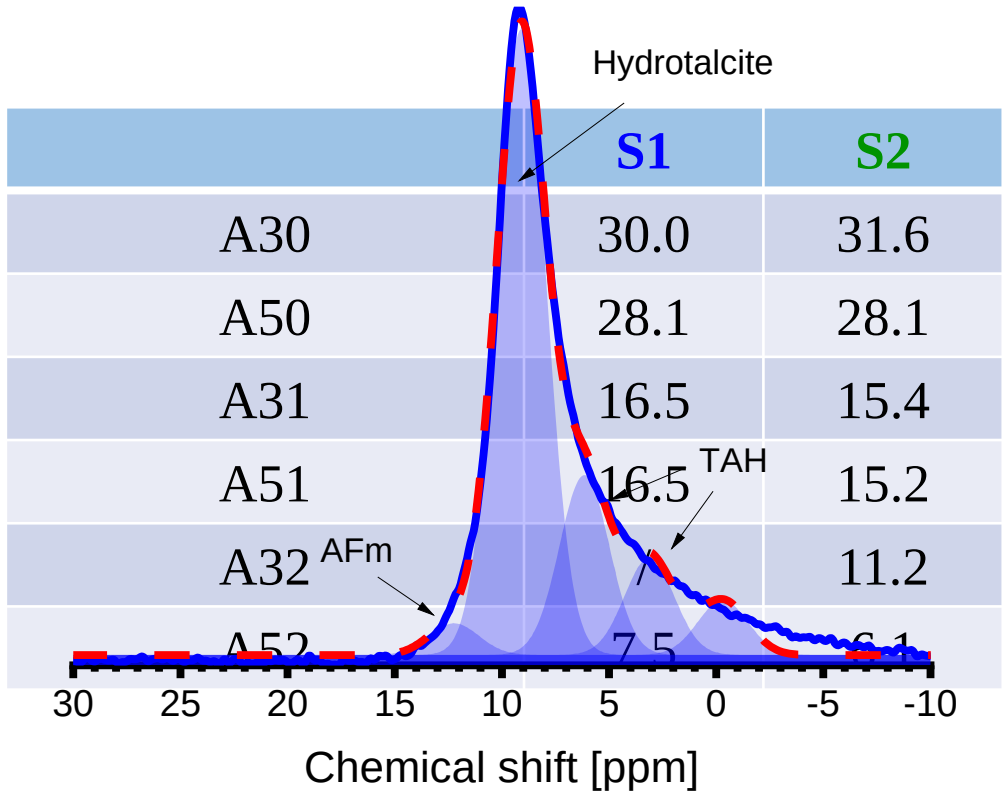

	S1	S2
A30	30.0	31.6
A50	28.1	28.1
A31	16.5	15.4
A51	16.5	15.2
A32	7	11.2
A52	7.5	6.1

$$\frac{2 \times (X_{Ca} + X_{Mg}) + X_K + X_{Na^*} - X_{Al}}{X_{Si^*} + X_{Al}}$$

hydrotalcite content depends on the silicate conc.

Reaction mechanism of alkali activated slag

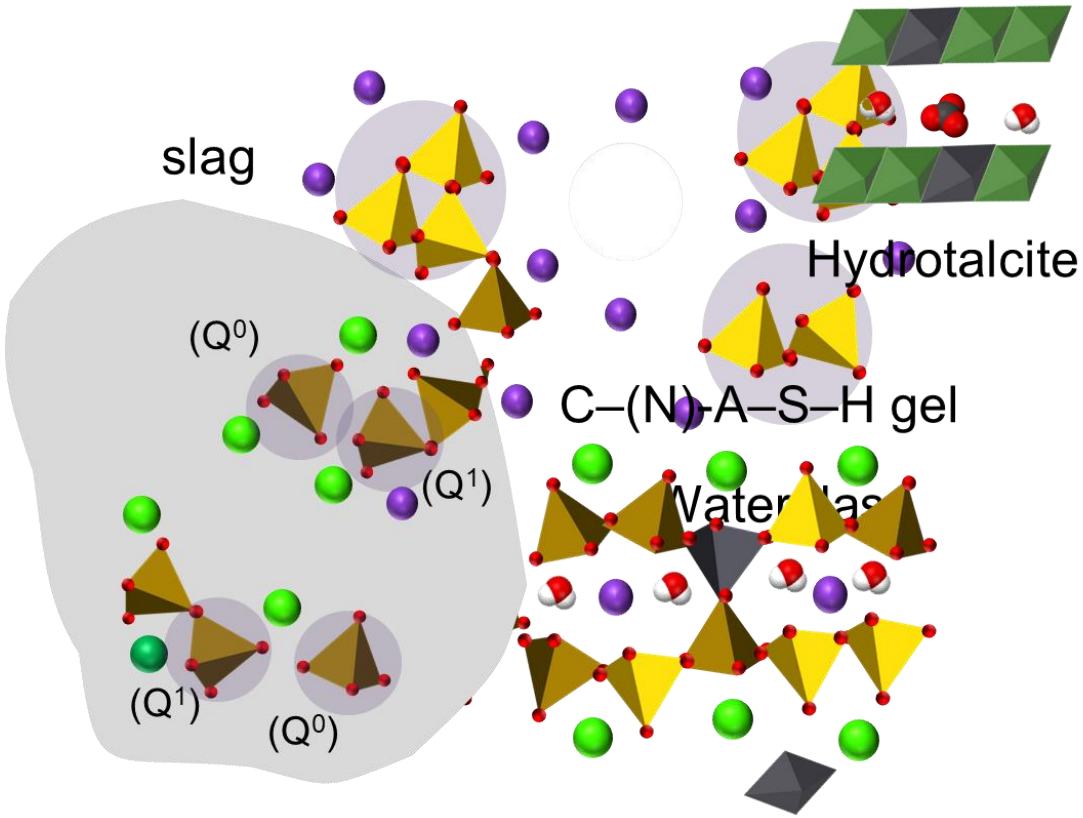

hydrolyse of Al-O-Si bonding

+

C-(N)-A-S-H gel at interface

reactivity

CONTENTS

1 Background

2 Methods

3 Results

4 Conclusions

Conclusions

1. The glass structure in slag and fly ash is mainly aluminosilicate, which was modelled by different models depending on the content of alkali cations. For fly ash, thermal history plays an important role in the structure as well.

2. The reactivity of both slag and fly ash by alkali activation is linearly correlated to the depolymerization degree of the glass structure (at ambient temperature). The correlation can be extended in the alkali activation system, in the absence of silicate anions from the activator.

Conclusions

3

Depolymerization degree of the glass structure determines the fate of Al, including the precipitation of hydrotalcite and the incorporation in C-A-S-H gel. The hydrolyse of Al-O-Si in the glass structure of slag is a key for the reactivity of slag by alkali activation, especially in the presence of silicate anions. In addition, the formed C-A-S-H gel in the vicinity in turn impedes the continuous dissolution of the aluminosilicate glass, which is another key for the reactivity of slag by alkali activation.

Thank you very much for your attention!

Questions?